machines

MDPI

Article

Distributed Fixed-Time Attitude Consensus Tracking Control for Multiple Rigid-Bodies Subject to Unknown Uncertainties

Sen Jiang [1], Zhong Yang [1,*], Yuxin Gao [1], Hao Xu [2] and Changliang Xu [1]

[1] College of Automation Engineering, Nanjing University of Aeronautics and Astronautics, Nanjing 211106, China; jiangsen1766@nuaa.edu.cn (S.J.); gaoyuxin@nuaa.edu.cn (Y.G.); xuchangliang@nuaa.edu.cn (C.X.)
[2] School of Mathematics and Physics, Anhui University of Technology, Ma'anshan 243032, China; ahaxuo@ahut.edu.cn
* Correspondence: yangzhong@nuaa.edu.cn

Abstract: This paper investigates the problem of fixed-time attitude consensus tracking control for a team of multiple rigid-bodies in the presence of unknown uncertainties. A robust exact distributed fixed-time observer is presented to estimate velocity state of the virtual-leader for the followers that could not directly access information of the virtual-leader. Subsequently, a novel distributed fixed-time consensus tracking control law is proposed, by which consensus tracking for a team of multiple rigid-bodies could be achieved in a fixed-time regardless of any initial system state. When the proposed control scheme is applied, effects of time-varying disturbances acting on each follower could drastically be attenuated. Analysis on stability of the closed-loop system is rigorously given and effectiveness of the proposed control scheme is verified by numerical simulations.

Keywords: fixed-time control; attitude consensus; multiple rigid-bodies; unknown uncertainties

Citation: Jiang, S.; Yang, Z.; Gao, Y.; Xu, H.; Xu, C. Distributed Fixed-Time Attitude Consensus Tracking Control for Multiple Rigid-Bodies Subject to Unknown Uncertainties. *Machines* **2022**, *10*, 383. https://doi.org/10.3390/machines10050383

Academic Editor: Dan Zhang

Received: 9 April 2022
Accepted: 11 May 2022
Published: 16 May 2022

1. Introduction

For a single rigid-body, there was multitudinous literature having investigated attitude control [1,2] or trajectory control [3–5]. However, when a task of high efficiency and large scale is required, an individual rigid-body (e.g., an aircraft or a robot) could not be unable to meet the specific requirements in some situations. Because of the high efficiency and the reliability of a multi-agent system (MASs), a group of multiple rigid-bodies can provide a new way to solve the complicated tasks. During the last two decades, cooperative control of multi-agent systems (MASs) has drawn increasing attention, which could be attributed to its widespread applications in various fields. For example, attitude and position synchronization for spacecraft formation flying [6–8], attitude consensus tracking for multiple rigid-bodies [9–11], distributed formation flying for a team of unmanned aerial vehicles (UAVs) [12–15], distributed formation control for a set of mobile robots [16,17], and cooperative guidance for a group of interceptors [18–20]. Among those works, the consensus control task, aiming at achieving an agreement among agents by using local information interaction, is often an elementary problem. Thus, numerous literature works have studied this problem recently.

In Ref. [21], an attitude consensus control scheme was proposed for a group of spacecraft attitude tracking without angular-velocity measurements. The control torques are naturally bounded, and the bounds of control torque could be arbitrarily prescribed through the control gains. In Ref. [22], the output consensus problem was investigated for a class of high-order nonlinear MASs. Based on a system state transformation, a distributed linear-like control law with a dynamic gain was proposed by using the agent and its neighbors output information. In addition, the orders of all considered agents could be different. In Ref. [23], a new distributed observer-type reduced-order output-feedback consensus control law was proposed for homogeneous linear MASs. System state consensus

was achieved, and the consensus conditions were presented. Regarding the consensus control problem, convergence speed is an important performance reflecting effectiveness of the proposed algorithm. The above-mentioned literature can only achieve asymptotic stability, which means that the convergence time is actually infinite. By contrast, finite-time stability implies faster settling-time and excellent robustness against various uncertainties.

Hence, a finite-time consensus control algorithm could attract more attention. In Ref. [24], a decentralized observer and a distributed observer were presented to estimate velocity state of each agent and acceleration of the leader, respectively. Based on the two finite-time observers, a distributed finite-time control law was proposed for multiple spacecraft formation flying with a virtual-leader. With the help of homogeneity theory, semi-global finite-time stability of the overall closed-loop system was rigorously proved. However, the robustness against uncertainties for each spacecraft is not taken into account. The authors of Ref. [25] proposed two robust distributed finite-time consensus protocols for MASs with double-integrator dynamics, in which leaderless and leader-following scenarios were considered, respectively. In the leader-following situation, a distributed finite-time observer was proposed to estimate velocity state of the leader. However, the presented control law is only for single-input single-output (SISO) systems. That is to say, for any node, the used mathematic model is a SISO system. In Ref. [26], the leader-following consensus problem was investigated for a class of second-order MASs. Based on a prescribed finite-time observer and a time-varying disturbance observer, a novel composite leader-following consensus control law was proposed. Both matched and mismatched disturbances could strongly be suppressed. It is worth pointing out that there is an obvious disadvantage of a finite-time consensus control law. If the initial condition is far away from the origin, the convergence speed of a finite-time algorithm is slower than an exponential convergence algorithm.

A solution to remove that drawback of a finite-time consensus control is the fixed-time consensus control. A recent review paper of this research orientation was given in Ref. [27]. In Ref. [28], based on a distributed fixed-time observer, two novel distributed fixed-time control laws were proposed for MASs with uncertainties acting on each agent. To mitigate the chattering effect, a boundary-layer method was employed, and a saturation-function was used to take the place of signum-function when the tracking errors enter the boundary-layer. Therefore, some performance reductions were paid for the expense of using the saturation-function. In Ref. [29], two fixed-time sliding-mode observers were presented at the beginning. Based on the two fixed-time observers, two distributed fixed-time attitude consensus control laws were proposed for a group of multiple spacecrafts. Required measurement of angular velocity was used in the first algorithm, whereas this requirement was removed in the second. With the aid of the two control laws, all spacecrafts are able to track a time-varying reference attitude, which is only available to a subset of the spacecrafts.

This work considers the fixed-time attitude consensus tracking control problem for a group of multiple rigid-bodies. Compared with the existing works of fixed-time consensus control law, the main contributions can be summarized as follows:

- A robust exact distributed fixed-time observer (REDFTO) is proposed to estimate velocity state of the virtual-leader. Settling-time of the dynamics of estimation error is independent of the initial conditions. The required computational burden of the REDFTO is less than some of the existing results [28,29], whereas fixed-time convergence of the estimation error to the origin could be guaranteed.
- Based on the presented REDFTO, a distributed fixed-time consensus tracking control (DFCTC) law is proposed for leader–follower MASs. Fixed-time convergence of the consensus tracking errors is proved by means of a modified back-stepping technique [30]. In the presence of lumped time-varying uncertainty acting on each agent, compared with the result [31], the settling-time and an ultimately bounded region are explicitly given.

This paper is organized as follows: preliminaries, some lemmas, problem statements and design objective are given in Section 2 after introduction in Section 1. In Section 3,

an REDFTO is proposed. Subsequently, a DFCTC law is proposed for leader-following MASs. Rigorous analysis on the fixed-time convergence is given by means of a modified back-stepping method. Numerical simulations are given to verify the proposed method in Section 4 following by the conclusions in Section 5.

2. Preliminaries and Problem Statements

2.1. Notations and Graph Theory

Some notations are given in the beginning. An n-elements natural number set Λ represents $\Lambda = \{1, 2, \cdots, n\}$. The set of all positive real numbers is represented by $\mathcal{R}^+$. $|\cdot|$ refers to the absolute value function. $\|\cdot\|$ represents the Euclidean norm of a vector. $\mathrm{sign}(\cdot)$ denotes the signum function. The Kronecker product between two matrices is expressed by the operator $\otimes$. For any column vector $\forall \boldsymbol{x} \in \mathcal{R}^n$, $\mathrm{sign}(\boldsymbol{x})$ denotes $\mathrm{sign}(\boldsymbol{x}) = [\mathrm{sign}(x_1), \cdots, \mathrm{sign}(x_n)]^T$. For a given real number $a \in \mathcal{R}^+$ and any column vector $\forall \boldsymbol{x} \in \mathcal{R}^n$, define $\mathrm{sgn}^a(\boldsymbol{x}) = [\mathrm{sgn}^a(x_1), \cdots, \mathrm{sgn}^a(x_n)]^T$ and $|x|^a = [|x_1|^a, \cdots, |x_n|^a]^T$, where $\mathrm{sgn}^a(x_i) = \mathrm{sign}(x_i)\,|x_i|^a, i \in \Lambda$. $\lambda_{\min}(\cdot)$ and $\lambda_{\max}(\cdot)$ represent the maximum eigenvalue and minimum eigenvalue of a matrix, respectively. $\mathbf{1}_n$ denotes $\mathbf{1}_n = [1, \cdots, 1]^T \in \mathcal{R}^n$, and $\mathbf{0}_n$ denotes $\mathbf{0}_n = [0, \cdots, 0]^T \in \mathcal{R}^n$. For any vector $\forall \boldsymbol{x} = [x_1, \cdots, x_n]^T \in \mathcal{R}^n$, its corresponding diagonal matrix is expressed as $\mathrm{diag}\{\boldsymbol{x}\} = \mathrm{diag}\{x_1, \cdots, x_n\}$. $\boldsymbol{x}^\times$ describes a skew-symmetric matrix $\boldsymbol{x}^\times \in \mathcal{R}^{3\times 3}$ as such

$$\boldsymbol{x}^\times = \begin{bmatrix} 0 & -x_3 & x_2 \\ x_3 & 0 & -x_1 \\ -x_2 & x_1 & 0 \end{bmatrix} \tag{1}$$

for any three-dimensional column vector $\forall \boldsymbol{x} = [x_1, x_2, x_3]^T \in \mathcal{R}^3$.

For an MAS, assuming that each agent is a node, information communication topology of the n-agents is denoted by a weighted graph $\mathcal{G} = \{\mathcal{V}, \mathcal{E}, \boldsymbol{A}\}$. $\mathcal{V} = \{\nu_i, i \in \Lambda\}$ is the set of vertices, $\mathcal{E} \subseteq \mathcal{V} \times \mathcal{V}$ is the set of edges, and $\boldsymbol{A} = [a_{ij}] \in \mathcal{R}^{n\times n}$ is the weighted adjacency matrix of graph $\mathcal{G}$ with nonnegative elements. For the i-th agent (node) ν_i, an edge in $\mathcal{G}$ is denoted by a two-element pair $(\nu_i, \nu_j) \in \mathcal{E}$, which indicates that there is an information exchange channel from node ν_i to node ν_j. All neighbors of node ν_i are described as a set $N_i = \{\nu_j : (\nu_i, \nu_j) \in \mathcal{E}\}$, and the out-degree of node ν_i is defined as $d_i = \sum_{j=1}^{n} a_{ij}$. For an edge $(\nu_i, \nu_j) \in \mathcal{E}$, the corresponding weighted element in matrix $\boldsymbol{A}$ is $a_{ij} > 0$; meanwhile, $(\nu_i, \nu_j) \notin \mathcal{E}$ also means $a_{ij} = 0$. Note that each diagonal element of the matrix $\boldsymbol{A}$ is equal to zero, i.e., $a_{ii} = 0$.

If $\mathcal{G}$ is undirected, it follows that $(\nu_i, \nu_j) \in \mathcal{E} \Leftrightarrow (\nu_j, \nu_i) \in \mathcal{E}$; it is also indicated that $a_{ij} = a_{ji}$, which means the weighted adjacency matrix $\boldsymbol{A}$ is a symmetric matrix. Laplacian matrix $\boldsymbol{L}$ of the weighted graph $\mathcal{G}$ is described as $\boldsymbol{L} = [l_{ij}] = \boldsymbol{D} - \boldsymbol{A}$, $\boldsymbol{L} \in \mathcal{R}^{n\times n}$, where degree matrix $\boldsymbol{D}$ of the graph $\mathcal{G}$ is denoted as $\boldsymbol{D} = \mathrm{diag}\{d_1, \cdots, d_n\}$. For any two nodes ν_i and ν_j, if there exists at least one path between them, the graph $\mathcal{G}$ is called a connected graph. It must be pointed out that only an undirected graph is considered in this paper.

If there exists a leader (or a virtual-leader) for the MAS, the leader could be labeled as 0. $\overline{\mathcal{G}}$ denotes an augmented graph with the vertex set $\overline{\mathcal{V}} = \mathcal{V} \bigcup \nu_0$. The information exchange channel between the leader and a follower is directed. There are only edges from the leader to some followers, but there is no edge from any follower to the leader. The connection weight between the leader and the u-th follower is denoted by $b_i, i \in \Lambda$. If the leader is connected to the i-th follower, $b_i > 0$; otherwise, $b_i = 0$. In addition, the weighted matrix $\boldsymbol{B}$ means $\boldsymbol{B} = \mathrm{diag}\{b_1, \cdots, b_n\}$.

2.2. Some Lemmas

Lemma 1 ([24]). *Given a real number $\alpha \in (0, 1]$, for $\forall x \in \mathcal{R}$, $\forall y \in \mathcal{R}$, the following inequality*

$$|\mathrm{sgn}^{\mathrm{ff}}(\mathrm{x}) - \mathrm{sgn}^{\mathrm{ff}}(\mathrm{y})| \leq 2^{1-\mathrm{ff}} |\mathrm{x} - \mathrm{y}|^{\mathrm{ff}} \tag{2}$$

holds.

Lemma 2 ([32]). *Provided some constants $c > 0$, $d > 0$, for $\forall x \in \mathcal{R}$, $\forall y \in \mathcal{R}$ and for $\forall \gamma > 0$, inequality*

$$|x|^c |y|^d \leq \frac{c}{c+d}\gamma |x|^{c+d} + \frac{d}{c+d}\gamma^{-\frac{c}{d}} |y|^{c+d} \tag{3}$$

holds.

Lemma 3 ([33]). *If a constant $0 < p < 1$, for $\forall x_i \in \mathbb{R}, i = 1, \cdots, m$, the following inequality holds:*

$$(|x_1| + \cdots + |x_m|)^p \leq |x_1|^p + \cdots + |x_m|^p \tag{4}$$

Lemma 4 ([24]). *If a constant $p > 1$, for $\forall x_i \in \mathbb{R}, i = 1, \cdots, m$, the following inequality holds:*

$$(|x_1| + \cdots + |x_m|)^p \leq m^{p-1}(|x_1|^p + \cdots + |x_m|^p) \tag{5}$$

Lemma 5 ([28]). *For a dynamic system $\dot{\boldsymbol{x}} = \boldsymbol{f}(t, \boldsymbol{x})$, $\boldsymbol{x} \in \mathcal{R}^n$, $\boldsymbol{x}(0) = \boldsymbol{x}_0$, if there exists a Lyapunov-function $V(\cdot)$ satisfying*

$$\dot{V}(\cdot) \leq -aV^{\alpha} - bV^{\beta},\ 0 < \alpha < 1, \beta > 1,\ a, b \in \mathcal{R}^+ \tag{6}$$

the state $\boldsymbol{x}$ will converge to zero in a fixed-time. This also implies that the settling-time $T(\boldsymbol{x}_0)$ is bounded by a constant $T_{\max}$, which could be expressed as

$$T(\boldsymbol{x}_0) \leq T_{\max} = \frac{1}{a}\frac{1}{1-\alpha} + \frac{1}{b}\frac{1}{\beta - 1} \tag{7}$$

2.3. Problem Statements

Consider a group of multiple rigid-bodies. Attitude dynamics for the i-th agent, which is similar to the model in Ref. [34], could be expressed by the Euler-angle representation as

$$\begin{cases} \dot{\boldsymbol{\omega}}_i = \boldsymbol{J}_i^{-1}[\boldsymbol{\tau}_i + \boldsymbol{\tau}_{di}(\cdot) - \boldsymbol{\omega}_i^{\times}\boldsymbol{J}_i\boldsymbol{\omega}_i] \\ \dot{\boldsymbol{\chi}}_i = \boldsymbol{Q}_i^{-1}\boldsymbol{\omega}_i \\ \boldsymbol{Q}_i = \begin{bmatrix} 1 & 0 & -\sin\theta_i \\ 0 & \cos\phi_i & \sin\phi_i\cos\theta_i \\ 0 & -\sin\phi_i & \cos\phi_i\cos\theta_i \end{bmatrix} \end{cases} \tag{8}$$

where $\boldsymbol{\chi}_i = [\phi_i, \theta_i, \psi_i]^T$ is the attitude vector. ϕ_i, θ_i and ψ_i are the rolling-angle, pitching-angle, and heading-angle, respectively. $\boldsymbol{J}_i \in \mathcal{R}^{3\times 3}$ is the inertial tensor matrix; $\boldsymbol{\omega}_i \in \mathcal{R}^3$ is angular velocity of the body-fixed frame with respect to the inertial frame. $\boldsymbol{\tau}_i = [\tau_{\phi,i}, \tau_{\theta,i}, \tau_{\psi,i}]^T$ is the control input torque, and $\boldsymbol{\tau}_{di}(\cdot)$ is the lumped uncertainty acting on the i-th rigid-body.

Set $\boldsymbol{x}_i = \boldsymbol{\chi}_i$, $\boldsymbol{v}_i = \dot{\boldsymbol{\chi}}_i$, and $\boldsymbol{u}_i = \boldsymbol{\Pi}_i^{-1}\boldsymbol{\tau}_i$, where $\boldsymbol{\Pi}_i = \boldsymbol{J}_i\boldsymbol{Q}_i$. Then, Equation (8) becomes

$$\begin{cases} \dot{\boldsymbol{x}}_i = \boldsymbol{v}_i \\ \dot{\boldsymbol{v}}_i = \boldsymbol{d}_i(\cdot) + \boldsymbol{u}_i,\ i = 1, \cdots, n \end{cases} \tag{9}$$

where $\boldsymbol{d}_i(\cdot) = \boldsymbol{\Pi}_i^{-1}\boldsymbol{\tau}_{di}(\cdot) - \boldsymbol{\Pi}_i^{-1}\boldsymbol{J}_i\dot{\boldsymbol{Q}}_i\dot{\boldsymbol{\chi}}_i - \boldsymbol{\Pi}_i^{-1}(\boldsymbol{Q}_i\dot{\boldsymbol{\chi}}_i)^{\times}\boldsymbol{\Pi}_i\dot{\boldsymbol{\chi}}_i$. In this second-order MAS, $\boldsymbol{x}_i \in \mathcal{R}^m$, $\boldsymbol{v}_i \in \mathcal{R}^m$ are the state vector and its first time derivative; $\boldsymbol{u}_i \in \mathcal{R}^m$ is the control input and $\boldsymbol{d}_i(\cdot) \in \mathcal{R}^m$ represents the uncertainty. The attitude command profile $[\boldsymbol{\chi}_0^T, \dot{\boldsymbol{\chi}}_0^T]^T$ could be denoted as a virtual-leader expressed as

$$\begin{cases} \dot{\boldsymbol{x}}_0 = \boldsymbol{v}_0 \\ \dot{\boldsymbol{v}}_0 = \boldsymbol{u}_0 \end{cases} \tag{10}$$

where $\boldsymbol{x}_0 = \boldsymbol{\chi}_0$, $\boldsymbol{v}_0 = \dot{\boldsymbol{\chi}}_0$, and $\boldsymbol{u}_0$ is angular acceleration of the virtual-leader. For the MAS (9) and (10), a definition about fixed-time consensus tracking should be presented as follows:

Definition 1 (Fixed-Time consensus tracking [27]). *Design a distributed control law* $\boldsymbol{u}_i = \boldsymbol{f}_u(\boldsymbol{x}_i, \boldsymbol{x}_j, \boldsymbol{v}_i, \boldsymbol{v}_j)$, $j \in N_i$ *for each follower* v_i, $i \in \Lambda$ *in* (9) *and* (10). *For any initial states* $[\boldsymbol{x}_i(t_0), \boldsymbol{v}_i(t_0)] \in \mathcal{R}^{2m}$ *and any bounded acceleration of the virtual-leader, if there exists a uniformly bounded time interval* $T_{\max} > 0$ *such that* $\boldsymbol{x}_i(t) = \boldsymbol{0}, \boldsymbol{v}_i(t) = \boldsymbol{0}, t > T_{\max}$, *the closed-loop MAS is said to be fixed-time consensus tracking. Moreover, the max settling-time* $T_{\max}$ *is independent of the initial states.*

Then, the attitude consensus tracking control objective for a team of rigid-bodies (9) could be stated as such. For the MAS (9) and (10), find a distributed control law that could make the attitude and its first time derivative of each rigid-body $[\boldsymbol{\chi}_i^T, \dot{\boldsymbol{\chi}}_i^T]^T$ follow a given command profile $[\boldsymbol{\chi}_0^T, \dot{\boldsymbol{\chi}}_0^T]^T$ in the presence of the lumped uncertainty $\boldsymbol{\tau}_{di}(\cdot)$ including internal perturbations and external disturbances. Moreover, the consensus tracking errors of each rigid-body could converge to a bounded region around the origin in a fixed-time.

3. Fixed-Time Consensus Tracking Control for Multiple Rigid-Bodies with Lumped Uncertainties

For the attitude consensus tracking control objective, two conditions, which are given as below, must be satisfied.

Assumption 1. *The augmented graph* $\overline{\mathcal{G}}$ *of the MAS* (9) *and* (10) *is connected. Moreover, acceleration of the virtual-leader is bounded, i.e.,* $\|\dot{\boldsymbol{v}}_0\| = \|\boldsymbol{u}_0\| \leq A_0$, *where the constant* A_0 *is a boundary.*

Assumption 2. *For each follower of the MAS* (9) *and* (10), *the uncertainty acting on each agent is bounded as* $\|\boldsymbol{d}_i(\cdot)\| \leq D_0$, $i \in \Lambda$, *where the constant* D_0 *is a boundary.*

Remark 1. *Indeed, the conditions required in Assumptions 1 and 2 are very common. In a practical engineering situation, the uncertainty may be parameter perturbations, unmodeled dynamics, or external disturbances including payload variations, environmental disturbance, etc. All of those kinds of uncertainties are bounded in the practical situations and so is acceleration of the virtual-leader. Consequently, applicability of the proposed control scheme could be enhanced.*

Because information of the virtual-leader v_0 could only be accessed by a subset of the followers, a REDFTO is proposed for the followers, which could not access information from the virtual-leader, to obtain an accurate estimation of velocity state of the virtual-leader v_0.

The REDFTO is presented as

$$\dot{\hat{\boldsymbol{v}}}_i = -c_1 \text{sign}(\boldsymbol{\varepsilon}_i) - c_2 \text{sgn}^{\beta}(\boldsymbol{\varepsilon}_i) \tag{11}$$

where $\boldsymbol{\varepsilon}_i = \sum_{j \in N_i} a_{ij}(\hat{\boldsymbol{v}}_i - \hat{\boldsymbol{v}}_j) + b_i(\hat{\boldsymbol{v}}_i - \boldsymbol{v}_0), i \in \Lambda, \beta > 1$ and $\hat{\boldsymbol{v}}_i$ is an estimation of $\boldsymbol{v}_0$ for the i-th agent. $c_1 \in \mathcal{R}^+$, $c_2 \in \mathcal{R}^+$ are two constants to be determined. The first main result of this paper could be summarized as:

Theorem 1. *Consider the observer* (11) *for the i-th agent. If the parameter* c_1 *and* c_2 *satisfy* $c_1 > \sqrt{n}A_0$, $c_2 > 0$, *the estimation error* $\bar{\boldsymbol{v}}_i = \hat{\boldsymbol{v}}_i - \boldsymbol{v}_0$ *will be steered to zero in a fixed-time.*

Proof. It is easily obtained that

$$\boldsymbol{\varepsilon}_i = \sum_{j \in N_i} a_{ij}(\hat{\boldsymbol{v}}_i - \hat{\boldsymbol{v}}_j) + b_i(\hat{\boldsymbol{v}}_i - \boldsymbol{v}_0) = \sum_{j=1}^{n} l_{ij}\bar{\boldsymbol{v}}_j + b_i\bar{\boldsymbol{v}}_i \tag{12}$$

In view of (11), the dynamic equation of $\bar{\boldsymbol{v}}_i$ is derived as

$$\dot{\bar{\boldsymbol{v}}}_i = -c_1 \text{sign}(\boldsymbol{\varepsilon}_i) - c_2 \text{sgn}^{\beta}(\boldsymbol{\varepsilon}_i) - \dot{\boldsymbol{v}}_0 \tag{13}$$

Choose a Lyapunov-function candidate as

$$V_0(\bar{\boldsymbol{v}}) = \frac{1}{2}\bar{\boldsymbol{v}}^T \boldsymbol{P}_0 \bar{\boldsymbol{v}} \tag{14}$$

where $\bar{\boldsymbol{v}} = [\bar{\boldsymbol{v}}_1^T, \cdots, \bar{\boldsymbol{v}}_n^T]^T$, $\boldsymbol{P}_0 = (\boldsymbol{L} + \boldsymbol{B}) \otimes \boldsymbol{I}_m$. Differentiating $V_0(\bar{\boldsymbol{v}})$ along (13) yields

$$\begin{aligned} \dot{V}_0 &= \bar{\boldsymbol{v}}^T \boldsymbol{P}_0 \dot{\bar{\boldsymbol{v}}} \\ &\leq -c_1 (\boldsymbol{P}_0 \bar{\boldsymbol{v}})^T \mathrm{sign}(\boldsymbol{P}_0 \bar{\boldsymbol{v}}) - c_2 (\boldsymbol{P}_0 \bar{\boldsymbol{v}})^T \mathrm{sgn}^{\beta}(\boldsymbol{P}_0 \bar{\boldsymbol{v}}) + \sqrt{n} A_0 \|\boldsymbol{P}_0 \bar{\boldsymbol{v}}\| \end{aligned} \tag{15}$$

where the Holder inequality is used. Note that

$$\begin{aligned} (\boldsymbol{P}_0 \bar{\boldsymbol{v}})^T \mathrm{sign}(\boldsymbol{P}_0 \bar{\boldsymbol{v}}) &\geq \|\boldsymbol{P}_0 \bar{\boldsymbol{v}}\| \\ (\boldsymbol{P}_0 \bar{\boldsymbol{v}})^T \mathrm{sgn}^{\beta}(\boldsymbol{P}_0 \bar{\boldsymbol{v}}) &\geq n^{\frac{1-\beta}{2}} m^{\frac{1-\beta}{2}} \|\boldsymbol{P}_0 \bar{\boldsymbol{v}}\|^{1+\beta} \end{aligned} \tag{16}$$

where Lemma 4 is used. Inserting (16) into (15) leads to

$$\begin{aligned} \dot{V}_0 &\leq -(c_1 - \sqrt{n}\, A_0) \|\boldsymbol{P}_0 \bar{\boldsymbol{v}}\| - c_2 n^{\frac{1-\beta}{2}} m^{\frac{1-\beta}{2}} \|\boldsymbol{P}_0 \bar{\boldsymbol{v}}\|^{1+\beta} \\ &\leq -(c_1 - \sqrt{n}\, A_0) \sqrt{\frac{2\lambda_{\min}(\boldsymbol{P}_0^2)}{\lambda_{\max}(\boldsymbol{P}_0)}} V_0^{\frac{1}{2}} - c_2 n^{\frac{1-\beta}{2}} m^{\frac{1-\beta}{2}} \left(\frac{2\lambda_{\min}(\boldsymbol{P}_0^2)}{\lambda_{\max}(\boldsymbol{P}_0)} \right)^{\frac{1+\beta}{2}} V_0^{\frac{1+\beta}{2}} \end{aligned} \tag{17}$$

From Lemma 5, it is easily known that, if $c_1 > \sqrt{n} A_0$, $c_2 > 0$, the estimation errors $\bar{\boldsymbol{v}}$ will converge to zero in a fixed-time T_1, which could be estimated as

$$\begin{aligned} T_1 &\leq \frac{2}{c_{d1}} + \frac{1}{c_{d2}} \frac{2}{\beta - 1} \\ c_{d1} &= (c_1 - \sqrt{n}\, A_0) \sqrt{\frac{2\lambda_{\min}(\boldsymbol{P}_0^2)}{\lambda_{\max}(\boldsymbol{P}_0)}},\ c_{d2} = c_2 n^{\frac{1-\beta}{2}} m^{\frac{1-\beta}{2}} \left(\frac{2\lambda_{\min}(\boldsymbol{P}_0^2)}{\lambda_{\max}(\boldsymbol{P}_0)} \right)^{\frac{1+\beta}{2}} \end{aligned} \tag{18}$$

This also implies that the settling-time T_1 is independent of the initial condition $\bar{\boldsymbol{v}}(0)$. The proof is complete. □

Remark 2. *For the leader-following consensus control problem, different distributed observers [24,25,28,29] are designed to estimate information of the leader. Different from the finite-time distributed observers [24,25], settling-time of the REDFTO (11) could be determined in advance. Compared with the fixed-time distributed observers [28,29], the REDFTO only used a higher-order term* $\mathrm{sgn}^{\beta}(\boldsymbol{\varepsilon}_i)$, $\beta > 1$ *and a discontinuous term* $\mathrm{sign}(\boldsymbol{\varepsilon}_i)$ *of the distributed estimation error* $\boldsymbol{\varepsilon}_i$. *However, considering about observers presented in Ref. [28,29], an additional lower-order term of the distributed estimation error was used. Hence, when the proposed REDFTO is employed, the utilization of hardware resources could to some extent be reduced. It must be pointed out that, for the follower with* $b_i > 0$, *the REDFTO is not needed in that the follower could access all states of the virtual-leader directly.*

With the help of REDFTO (11), a DFCTC law for MAS (9) and (10) is proposed as such

$$\begin{aligned} \boldsymbol{u}_i = &-c_4 \mathrm{sgn}^{2\alpha_1 - 1} \left\{ \mathrm{sgn}^{\frac{1}{\alpha_1}} [(\boldsymbol{v}_i - \hat{\boldsymbol{v}}_i) + \lambda \mathrm{sgn}^{\alpha_2}(\boldsymbol{\epsilon}_i)] + c_3^{\frac{1}{\alpha_1}} \boldsymbol{\epsilon}_i \right\} \\ &- c_5 \mathrm{sgn}^{\alpha_1 + \alpha_2 - 1} \left\{ \mathrm{sgn}^{\frac{1}{\alpha_1}} [(\boldsymbol{v}_i - \hat{\boldsymbol{v}}_i) + \lambda \mathrm{sgn}^{\alpha_2}(\boldsymbol{\epsilon}_i)] + c_3^{\frac{1}{\alpha_1}} \boldsymbol{\epsilon}_i \right\} \\ &- \lambda \alpha_2 \, \mathrm{diag}\{|\boldsymbol{\epsilon}_i|^{\alpha_2 - 1}\} \boldsymbol{\eta}_i \end{aligned} \tag{19}$$

where $\boldsymbol{\epsilon}_i = \sum_{j\in N_i} a_{ij}(\boldsymbol{x}_i - \boldsymbol{x}_j) + b_i(\boldsymbol{x}_i - \boldsymbol{x}_0)$, $\boldsymbol{\eta}_i = \sum_{j\in N_i} a_{ij}(\boldsymbol{v}_i - \boldsymbol{v}_j) + b_i(\boldsymbol{v}_i - \boldsymbol{v}_0)$, and $0 < \alpha_1 < 1$. Set the consensus tracking errors $\tilde{\boldsymbol{x}}_i$, $\tilde{\boldsymbol{v}}_i$ for the i-th agent as $\tilde{\boldsymbol{x}}_i = \boldsymbol{x}_i - \boldsymbol{x}_0$, $\tilde{\boldsymbol{v}}_i = \boldsymbol{v}_i - \boldsymbol{v}_0$ respectively, and introduce an auxiliary variable $\boldsymbol{w}_i = \tilde{\boldsymbol{v}}_i + \lambda\,\mathrm{sgn}^{\alpha_2}(\boldsymbol{\epsilon}_i)$, where $\alpha_2 > 1$.

When $t > T_1$, from Theorem 1, it is proved that $\hat{\boldsymbol{v}}_i = \boldsymbol{v}_0, i \in \Lambda$. Hence, it follows that $\tilde{\boldsymbol{v}}_i = \boldsymbol{v}_i - \boldsymbol{v}_0 = \boldsymbol{v}_i - \hat{\boldsymbol{v}}_i$. Then, during the time $t > T_1$, stability analysis for the closed-loop system (9), (10) and (19) is carried out via a modified back-stepping method, which could be divided into two steps.

Step 1. Consider a Lyapunov-function candidate

$$V_1(\tilde{\boldsymbol{x}}) = \frac{1}{2}\tilde{\boldsymbol{x}}^T\boldsymbol{P}_0\tilde{\boldsymbol{x}} \tag{20}$$

where $\tilde{\boldsymbol{x}} = [\tilde{\boldsymbol{x}}_1^T, \cdots, \tilde{\boldsymbol{x}}_n^T]^T \in \mathcal{R}^{mn}$, the matrix $\boldsymbol{P}_0$ is defined in (14). Similarly, set $\tilde{\boldsymbol{v}} = [\tilde{\boldsymbol{v}}_1^T, \cdots, \tilde{\boldsymbol{v}}_n^T]^T \in \mathcal{R}^{mn}$, $\boldsymbol{w} = [\boldsymbol{w}_1^T, \cdots, \boldsymbol{w}_n^T]^T \in \mathcal{R}^{mn}$, $\boldsymbol{\epsilon} = [\boldsymbol{\epsilon}_1^T, \cdots, \boldsymbol{\epsilon}_n^T]^T \in \mathcal{R}^{mn}$, and $\boldsymbol{u} = [\boldsymbol{u}_1^T, \cdots, \boldsymbol{u}_n^T]^T \in \mathcal{R}^{mn}$. Taking the first time derivative of V_1 yields

$$\dot{V}_1 = \tilde{\boldsymbol{x}}^T\boldsymbol{P}_0\tilde{\boldsymbol{v}} = \tilde{\boldsymbol{x}}^T\boldsymbol{P}_0\boldsymbol{w} - \lambda\tilde{\boldsymbol{x}}^T\boldsymbol{P}_0\mathrm{sgn}^{\alpha_2}(\boldsymbol{\epsilon}) \tag{21}$$

Choosing a virtual control $\boldsymbol{w}^* = -c_3\mathrm{sgn}^{\alpha_1}(\boldsymbol{\epsilon})$, (21) becomes

$$\begin{aligned}
\dot{V}_1 &= -c_3\boldsymbol{\epsilon}^T\mathrm{sgn}^{\alpha_1}(\boldsymbol{\epsilon}) - \lambda\boldsymbol{\epsilon}^T\mathrm{sgn}^{\alpha_2}(\boldsymbol{\epsilon}) + \boldsymbol{\epsilon}^T(\boldsymbol{w} - \boldsymbol{w}^*) \\
&\le -c_3\boldsymbol{\epsilon}^T\mathrm{sgn}^{\alpha_1}(\boldsymbol{\epsilon}) - \lambda\boldsymbol{\epsilon}^T\mathrm{sgn}^{\alpha_2}(\boldsymbol{\epsilon}) + 2^{1-\alpha_1}\sum_{i=1}^{n}\sum_{k=1}^{m}|\epsilon_{ik}|\,|\xi_{ik}|^{\alpha_1} \\
&\le -c_3\boldsymbol{\epsilon}^T\mathrm{sgn}^{\alpha_1}(\boldsymbol{\epsilon}) - \lambda\boldsymbol{\epsilon}^T\mathrm{sgn}^{\alpha_2}(\boldsymbol{\epsilon}) + \hat{c}_{31}\boldsymbol{\epsilon}^T\mathrm{sgn}^{\alpha_1}(\boldsymbol{\epsilon}) + \hat{c}_{41}\boldsymbol{\xi}^T\mathrm{sgn}^{\alpha_1}(\boldsymbol{\xi}) \\
\hat{c}_{31} &= \frac{2^{1-\alpha_1}}{1+\alpha_1}, \hat{c}_{41} = \frac{2^{1-\alpha_1}\alpha_1}{1+\alpha_1}
\end{aligned} \tag{22}$$

where Lemma 2 is used.

Step 2. Choose the following Lyapunov-function candidate:

$$\begin{aligned}
V(\cdot) &= V_1(\cdot) + V_2(\cdot) \\
V_2(\cdot) &= \sum_{i=1}^{n} V_{2i},\ V_{2i} = \sum_{k=1}^{m} V_{2i,k}(\cdot) \\
V_{2i,k}(\cdot) &= \int_{w_{ik}^*}^{w_{ik}} \mathrm{sgn}^{2-\alpha_1}\left(\mathrm{sgn}^{\frac{1}{\alpha_1}}(\iota) - \mathrm{sgn}^{\frac{1}{\alpha_1}}(w_{ik}^*)\right)\mathrm{d}\iota
\end{aligned} \tag{23}$$

From the third line of (23), the first time derivative of $V_{2i,k}(\cdot)$ can be expressed as

$$\begin{aligned}
\dot{V}_{2i,k}(\cdot) &= \mathrm{sgn}^{2-\alpha_1}(\xi_{ik})\dot{w}_{ik} + (2-\alpha_1)c_3^{\frac{1}{\alpha_1}}\dot{\epsilon}_{ik}\int_{w_{ik}^*}^{w_{ik}}\left|\mathrm{sgn}^{\frac{1}{\alpha_1}}(\iota) - \mathrm{sgn}^{\frac{1}{\alpha_1}}(w_{ik}^*)\right|^{1-\alpha_1}\mathrm{d}\iota \\
&\le \mathrm{sgn}^{2-\alpha_1}(\xi_{ik})\dot{w}_{ik} + (2-\alpha_1)2^{1-\alpha_1}c_3^{\frac{1}{\alpha_1}}|\xi_{ik}|\dot{\epsilon}_{ik}
\end{aligned} \tag{24}$$

where Lemma 1 and $\xi_{ik} = \mathrm{sgn}^{\frac{1}{\alpha_1}}(w_{ik}) - \mathrm{sgn}^{\frac{1}{\alpha_1}}(w_{ik}^*)$ are used. Introduce two constants: $d_m = \max_{i\in\Lambda}\left\{b_i + \sum_{j\in N_i} a_{ij}\right\}$, $a_m = \max_{i,j\in\Lambda}\{a_{ij}\}$. It is easily observed that

$$\begin{aligned}
\dot{\epsilon}_{ik} &= \left[\sum_{j\in N_i} a_{ij}(w_{ik} - w_{jk}) + b_i w_{ik}\right] \\
&\quad - \lambda\left[\sum_{j\in N_i} a_{ij}(\mathrm{sgn}^{\alpha_2}(\epsilon_{ik}) - \mathrm{sgn}^{\alpha_2}(\epsilon_{jk})) + b_i\mathrm{sgn}^{\alpha_2}(\epsilon_{ik})\right] \\
&\le d_m|w_{ik}| + a_m\sum_{l=1}^{n}|w_{lk}| + \lambda\left(d_m|\epsilon_{ik}|^{\alpha_2} + a_m\sum_{l=1}^{n}|\epsilon_{lk}|^{\alpha_2}\right)
\end{aligned} \tag{25}$$

Applying (25) into (24) yields

$$\begin{aligned}\dot{V}_{2i,k}(\cdot) \leq \operatorname{sgn}^{2-\alpha_1}(\xi_{ik})\dot{w}_{ik} + (2-\alpha_1)2^{1-\alpha_1}(c_3^{\frac{1}{\alpha_1}} d_m|w_{ik}|\,|\xi_{ik}| \\ + c_3^{\frac{1}{\alpha_1}} a_m|\xi_{ik}|\sum_{l=1}^{n}|w_{lk}| + c_3^{\frac{1}{\alpha_1}}\lambda d_m|\epsilon_{ik}|^{\alpha_2}|\xi_{ik}| + c_3^{\frac{1}{\alpha_1}}\lambda a_m|\xi_{ik}|\sum_{l=1}^{n}|\epsilon_{lk}|^{\alpha_2}\Big)\end{aligned} \tag{26}$$

According to Lemma 2, it is easily obtained that

$$\begin{aligned} & d_m c_3^{\frac{1}{\alpha_1}}|w_{ik}|\,|\xi_{ik}| \\ & \leq d_m c_3^{\frac{1}{\alpha_1}}|w_{ik}-w_{ik}^*|\,|\xi_{ik}| + d_m c_3^{1+\frac{1}{\alpha_1}}|\epsilon_{ik}|^{\alpha_1}\,|\xi_{ik}| \\ & \leq d_m 2^{1-\alpha_1} c_3^{\frac{1}{\alpha_1}}|\xi_{ik}|^{\alpha_1+1} + \frac{d_m\alpha_1}{\alpha_1+1}|\epsilon_{ik}|^{\alpha_1+1} + \frac{d_m}{\alpha_1+1}c_3^{\alpha_1+1}|\xi_{ik}|^{\alpha_1+1}\end{aligned} \tag{27}$$

In the same vein, it is also obtained that

$$\begin{aligned} & a_m c_3^{\frac{1}{\alpha_1}}|\xi_{ik}|\sum_{l=1}^{n}|w_{lk}| \\ & \leq a_m 2^{1-\alpha_1} c_3^{\frac{1}{\alpha_1}}\frac{\alpha_1}{\alpha_1+1}\sum_{l=1}^{n}|\xi_{lk}|^{\alpha_1+1} + n\,a_m 2^{1-\alpha_1}c_3^{\frac{1}{\alpha_1}}\frac{1}{\alpha_1+1}|\xi_{ik}|^{\alpha_1+1} \\ & \quad + \frac{a_m\alpha_1}{\alpha_1+1}\sum_{l=1}^{n}|\epsilon_{lk}|^{\alpha_1+1} + \frac{n\,a_m}{\alpha_1+1}c_3^{\alpha_1+1}|\xi_{ik}|^{\alpha_1+1} \\ & \lambda d_m c_3^{\frac{1}{\alpha_1}}|\epsilon_{ik}|^{\alpha_2}|\xi_{ik}| \leq d_m\frac{\alpha_2}{\alpha_2+1}|\epsilon_{ik}|^{\alpha_2+1} + \lambda^{\alpha_2}d_m\frac{1}{\alpha_2+1}c_3^{\frac{\alpha_2}{\alpha_1}}|\xi_{ik}|^{\alpha_2+1} \\ & \lambda a_m c_3^{\frac{1}{\alpha_1}}|\xi_{ik}|\sum_{l=1}^{n}|\epsilon_{lk}|^{\alpha_2} \leq a_m\frac{\alpha_2}{\alpha_2+1}\sum_{l=1}^{n}|\epsilon_{lk}|^{\alpha_2+1} + n\,\lambda^{\alpha_2}a_m\frac{1}{\alpha_2+1}c_3^{\frac{\alpha_2}{\alpha_1}}|\xi_{ik}|^{\alpha_2+1}\end{aligned} \tag{28}$$

Inserting (27) and (28) into (26) results in

$$\begin{aligned}\dot{V}_{2i,k}(\cdot) \leq \operatorname{sgn}^{2-\alpha_1}(\xi_{ik})\dot{w}_{ik} \\ + \hat{c}_{32}|\epsilon_{ik}|^{\alpha_1+1} + \hat{c}_{33}\sum_{l=1}^{n}|\epsilon_{lk}|^{\alpha_1+1} + \hat{c}_{34}|\epsilon_{ik}|^{\alpha_2+1} + \hat{c}_{35}\sum_{l=1}^{n}|\epsilon_{lk}|^{\alpha_2+1} \\ + \hat{c}_{42}|\xi_{ik}|^{\alpha_1+1} + \hat{c}_{43}\sum_{l=1}^{n}|\xi_{lk}|^{\alpha_1+1} + \hat{c}_{44}|\xi_{ik}|^{\alpha_2+1}\end{aligned} \tag{29}$$

where

$$\begin{aligned}\hat{c}_{32} &= (2-\alpha_1)2^{1-\alpha_1}\frac{d_m\alpha_1}{\alpha_1+1},\ \hat{c}_{33} = (2-\alpha_1)2^{1-\alpha_1}\frac{a_m\alpha_1}{\alpha_1+1} \\ \hat{c}_{34} &= (2-\alpha_1)2^{1-\alpha_1}d_m\frac{\alpha_2}{\alpha_2+1},\ \hat{c}_{35} = (2-\alpha_1)2^{1-\alpha_1}a_m\frac{\alpha_2}{\alpha_2+1} \\ \hat{c}_{42} &= (2-\alpha_1)2^{1-\alpha_1}\Big(d_m 2^{1-\alpha_1}c_3^{\frac{1}{\alpha_1}} + \frac{d_m}{\alpha_1+1}c_3^{\alpha_1+1} \\ & \quad + n\,a_m 2^{1-\alpha_1}c_3^{\frac{1}{\alpha_1}}\frac{1}{\alpha_1+1} + \frac{n\,a_m}{\alpha_1+1}c_3^{\alpha_1+1}\Big) \\ \hat{c}_{43} &= (2-\alpha_1)2^{1-\alpha_1}a_m 2^{1-\alpha_1}c_3^{\frac{1}{\alpha_1}}\frac{\alpha_1}{\alpha_1+1} \\ \hat{c}_{44} &= (2-\alpha_1)2^{1-\alpha_1}\Big(\lambda^{\alpha_2}d_m\frac{1}{\alpha_2+1}c_3^{\frac{\alpha_2}{\alpha_1}} + n\,\lambda^{\alpha_2}a_m\frac{1}{\alpha_2+1}c_3^{\frac{\alpha_2}{\alpha_1}}\Big)\end{aligned} \tag{30}$$

Therefore, it can be derived from (29) that

$$\begin{aligned}\dot{V}_{2i}(\cdot) \leq\ & \mathrm{sgn}^{2-\alpha_1}(\boldsymbol{\xi}_i^T)\dot{\boldsymbol{w}}_i + \hat{c}_{32}\boldsymbol{\epsilon}_i^T\mathrm{sgn}^{\alpha_1}(\boldsymbol{\epsilon}_i) \\ & + \hat{c}_{33}\sum_{l=1}^{n}\boldsymbol{\epsilon}_l^T\mathrm{sgn}^{\alpha_1}(\boldsymbol{\epsilon}_l) + \hat{c}_{34}\boldsymbol{\epsilon}_i^T\mathrm{sgn}^{\alpha_2}(\boldsymbol{\epsilon}_i) + \hat{c}_{35}\sum_{l=1}^{n}\boldsymbol{\epsilon}_l^T\mathrm{sgn}^{\alpha_2}(\boldsymbol{\epsilon}_l) \\ & + \hat{c}_{42}\boldsymbol{\xi}_i^T\mathrm{sgn}^{\alpha_1}(\boldsymbol{\xi}_i) + \hat{c}_{43}\sum_{l=1}^{n}\boldsymbol{\xi}_l^T\mathrm{sgn}^{\alpha_1}(\boldsymbol{\xi}_l) + \hat{c}_{44}\boldsymbol{\xi}_i^T\mathrm{sgn}^{\alpha_2}(\boldsymbol{\xi}_i)\end{aligned} \tag{31}$$

This also means that

$$\begin{aligned}\dot{V}_2(\cdot) \leq\ & \mathrm{sgn}^{2-\alpha_1}(\boldsymbol{\xi}^T)\dot{\boldsymbol{w}} + (\hat{c}_{32} + n\,\hat{c}_{33})\boldsymbol{\epsilon}^T\mathrm{sgn}^{\alpha_1}(\boldsymbol{\epsilon}) \\ & + (\hat{c}_{34} + n\,\hat{c}_{35})\boldsymbol{\epsilon}^T\mathrm{sgn}^{\alpha_2}(\boldsymbol{\epsilon}) + (\hat{c}_{42} + n\,\hat{c}_{43})\boldsymbol{\xi}^T\mathrm{sgn}^{\alpha_1}(\boldsymbol{\xi}) + \hat{c}_{44}\boldsymbol{\xi}^T\mathrm{sgn}^{\alpha_2}(\boldsymbol{\xi})\end{aligned} \tag{32}$$

Choose a fixed-time control law as

$$\boldsymbol{u} = -c_4\,\mathrm{sgn}^{2\alpha_1-1}(\boldsymbol{\xi}) - c_5\,\mathrm{sgn}^{\alpha_1+\alpha_2-1}(\boldsymbol{\xi}) - \lambda\alpha_2\,\mathrm{diag}\{|\boldsymbol{\epsilon}|^{\alpha_2-1}\}\boldsymbol{P}_0\tilde{\boldsymbol{v}} \tag{33}$$

where c_4, c_5, λ are some constants to be determined later. Then, the second main result of this paper is presented as follows:

Theorem 2. *Consider the closed-loop system (9), (10) and (19), during the time $t > T_1$. Provided that Assumptions 1 and 2 are satisfied, there exist some constants c_0, c_3, c_4, and λ such that the consensus tracking errors of the closed-loop system are bounded. Furthermore, the consensus tracking error of each agent will be steered into a set $\mathcal{S}_i$ in a fixed-time. The set $\mathcal{S}_i$, in which the origin is included, is expressed as*

$$\begin{aligned}\mathcal{S}_i = \Bigg\{ & (\tilde{\boldsymbol{x}}_i, \tilde{\boldsymbol{v}}_i) : \|\tilde{\boldsymbol{x}}_i\| = \|\boldsymbol{x}_i - \boldsymbol{x}_0\| \leq \sqrt{\frac{2n\,d_{s2}}{\zeta}}, \\ & \|\tilde{\boldsymbol{v}}_i\| = \|\boldsymbol{v}_i - \boldsymbol{v}_0\| \leq \left(2^{\frac{(2-\alpha_1)(1-\alpha_1)}{2}} + c_3 c_v^{\frac{\alpha_1}{2}}\right)(mn)^{\frac{1-\alpha_1}{2}} d_{s2}^{\frac{\alpha_1}{2}} + \lambda\, c_v^{\frac{\alpha_2}{2}} d_{s2}^{\frac{\alpha_2}{2}} \Bigg\}\end{aligned} \tag{34}$$

where $\zeta = \min\{a_{ij}, b_i,\ i,j \in \Lambda\}$, $c_v = \min\left\{\frac{2\lambda_{\min}(\boldsymbol{P}_0^2)}{\lambda_{\max}(\boldsymbol{P}_0)}, 2^{\alpha_1-1}\right\}$, and $d_{s2} = \frac{1}{c_v}\left(\frac{2\rho}{c_0}\right)^{\frac{2}{2\alpha_1-1}}$, $\rho = \sqrt{n}\,(D_0 + A_0)$. In addition, the settling-time is bounded by a constant T_2

$$\begin{aligned}T_2 &\leq \frac{1}{c_{d3}}\frac{2}{1-\alpha_1} + \frac{1}{c_{d4}}\frac{2}{\alpha_2 - 1} \\ c_{d3} &= \frac{c_0}{2}c_v^{\frac{\alpha_1+1}{2}}\quad c_{d4} = c_0\,(mn)^{\frac{1-\alpha_2}{2}}c_v^{\frac{\alpha_2+1}{2}}\end{aligned} \tag{35}$$

Proof. The following proof is divided into two parts: (1) Convergence of the consensus tracking errors is analyzed; (2) The globally attractive region is pointed out, and hence an estimation for the tracking error boundary of each agent could be presented.

1. Combining (22) with (32) and using (33) lead to

$$\begin{aligned}\dot{V}(\cdot) \leq\ & \mathrm{sgn}^{2-\alpha_1}(\boldsymbol{\xi}^T)(\boldsymbol{d} - \boldsymbol{1}_n \otimes \dot{\boldsymbol{v}}_0) \\ & - (c_3 - \hat{c}_{31} - \hat{c}_{32} - n\,\hat{c}_{33})\boldsymbol{\epsilon}^T\mathrm{sgn}^{\alpha_1}(\boldsymbol{\epsilon}) - (\lambda - \hat{c}_{34} - n\,\hat{c}_{35})\boldsymbol{\epsilon}^T\mathrm{sgn}^{\alpha_2}(\boldsymbol{\epsilon}) \\ & - (c_4 - \hat{c}_{41} - \hat{c}_{42} - n\,\hat{c}_{43})\boldsymbol{\xi}^T\mathrm{sgn}^{\alpha_1}(\boldsymbol{\xi}) - (c_5 - \hat{c}_{44})\boldsymbol{\xi}^T\mathrm{sgn}^{\alpha_2}(\boldsymbol{\xi})\end{aligned} \tag{36}$$

where $\boldsymbol{d} = [\boldsymbol{d}_1, \cdots, \boldsymbol{d}_n]^T \in \mathcal{R}^{mn}$. Choose the parameters c_3, c_4, c_5 and λ as such

$$\begin{aligned} c_3 &\geq \hat{c}_{31} + \hat{c}_{32} + n\,\hat{c}_{33} + c_0 \\ c_4 &\geq \hat{c}_{41} + \hat{c}_{42} + n\,\hat{c}_{43} + c_0 \\ c_5 &\geq \hat{c}_{44} + c_0,\ \lambda \geq \hat{c}_{34} + n\,\hat{c}_{35} + c_0 \end{aligned} \tag{37}$$

where c_0 is an arbitrary positive constant determined by the designer. Thus, (36) becomes

$$\begin{aligned} \dot{V}(\cdot) &\leq \mathrm{sgn}^{2-\alpha_1}(\boldsymbol{\xi}^T)(\boldsymbol{d} - \mathbf{1}_n \otimes \dot{v}_0) - c_0\left[\boldsymbol{\epsilon}^T \mathrm{sgn}^{\alpha_1}(\boldsymbol{\epsilon}) + \boldsymbol{\xi}^T \mathrm{sgn}^{\alpha_1}(\boldsymbol{\xi})\right] \\ &\quad - c_0\left[\boldsymbol{\epsilon}^T \mathrm{sgn}^{\alpha_2}(\boldsymbol{\epsilon}) + \boldsymbol{\xi}^T \mathrm{sgn}^{\alpha_2}(\boldsymbol{\xi})\right] \\ &\leq \rho\left(\boldsymbol{\epsilon}^T\boldsymbol{\epsilon} + \boldsymbol{\xi}^T\boldsymbol{\xi}\right)^{\frac{2-\alpha_1}{2}} - c_0\left(\boldsymbol{\epsilon}^T\boldsymbol{\epsilon} + \boldsymbol{\xi}^T\boldsymbol{\xi}\right)^{\frac{\alpha_1+1}{2}} - c_0\,(mn)^{\frac{1-\alpha_2}{2}}\left(\boldsymbol{\epsilon}^T\boldsymbol{\epsilon} + \boldsymbol{\xi}^T\boldsymbol{\xi}\right)^{\frac{\alpha_2+1}{2}} \end{aligned} \tag{38}$$

where $\rho = \sqrt{n}\,(D_0 + A_0)$. Considering $\lambda_{\min}(\boldsymbol{P}_0^2)\|\tilde{\boldsymbol{x}}\|^2 \leq \boldsymbol{\epsilon}^T\boldsymbol{\epsilon}$, $2V_1(\boldsymbol{x}) \leq \lambda_{\max}(\boldsymbol{P}_0)\|\tilde{\boldsymbol{x}}\|^2$ and $V_2(\cdot) \leq 2^{1-\alpha_1}\boldsymbol{\xi}^T\boldsymbol{\xi}$, it follows that

$$\begin{aligned} \frac{2\lambda_{\min}(\boldsymbol{P}_0^2)}{\lambda_{\max}(\boldsymbol{P}_0)} V_1(\cdot) \leq \boldsymbol{\epsilon}^T\boldsymbol{\epsilon},\ 2^{\alpha_1-1}V_2(\cdot) \leq \boldsymbol{\xi}^T\boldsymbol{\xi} \\ c_v V(\cdot) \leq \left(\boldsymbol{\epsilon}^T\boldsymbol{\epsilon} + \boldsymbol{\xi}^T\boldsymbol{\xi}\right) \end{aligned} \tag{39}$$

where $c_v = \min\left\{\frac{2\lambda_{\min}(\boldsymbol{P}_0^2)}{\lambda_{\max}(\boldsymbol{P}_0)}, 2^{\alpha_1-1}\right\}$. Inserting the second line of (39) into (38) yields

$$\begin{aligned} \dot{V}(\cdot) \leq -\frac{c_0}{2}\left[\left(\boldsymbol{\epsilon}^T\boldsymbol{\epsilon} + \boldsymbol{\xi}^T\boldsymbol{\xi}\right)^{\frac{2\alpha_1-1}{2}} - \frac{2\rho}{c_0}\right]\left(\boldsymbol{\epsilon}^T\boldsymbol{\epsilon} + \boldsymbol{\xi}^T\boldsymbol{\xi}\right)^{\frac{2-\alpha_1}{2}} \\ - \frac{c_0}{2}c_v^{\frac{\alpha_1+1}{2}}V^{\frac{\alpha_1+1}{2}} - c_0\,(mn)^{\frac{1-\alpha_2}{2}}c_v^{\frac{\alpha_2+1}{2}}V^{\frac{\alpha_2+1}{2}} \end{aligned} \tag{40}$$

When $\left(\boldsymbol{\epsilon}^T\boldsymbol{\epsilon} + \boldsymbol{\xi}^T\boldsymbol{\xi}\right)^{\frac{2\alpha_1-1}{2}} > \frac{2\rho}{c_0}$, (40) becomes

$$\dot{V}(\cdot) \leq -\frac{c_0}{2}c_v^{\frac{\alpha_1+1}{2}}V^{\frac{\alpha_1+1}{2}} - c_0\,(mn)^{\frac{1-\alpha_2}{2}}c_v^{\frac{\alpha_2+1}{2}}V^{\frac{\alpha_2+1}{2}} \tag{41}$$

which indicates that $[\boldsymbol{\epsilon}^T, \boldsymbol{\xi}^T]^T$ will converge to the set $\Delta_1 = \left\{(\boldsymbol{\epsilon}, \boldsymbol{\xi}) : \left(\boldsymbol{\epsilon}^T\boldsymbol{\epsilon} + \boldsymbol{\xi}^T\boldsymbol{\xi}\right)^{\frac{2\alpha_1-1}{2}} \leq \frac{2\rho}{c_0}\right\}$ in a fixed-time T_2. Furthermore, the settling-time is bounded by

$$\begin{aligned} T_2 &\leq \frac{1}{c_{d3}}\frac{2}{1-\alpha_1} + \frac{1}{c_{d4}}\frac{2}{\alpha_2 - 1} \\ c_{d3} &= \frac{c_0}{2}c_v^{\frac{\alpha_1+1}{2}}\ c_{d4} = c_0\,(mn)^{\frac{1-\alpha_2}{2}}c_v^{\frac{\alpha_2+1}{2}} \end{aligned} \tag{42}$$

2. Consider a set $\Delta_2 = \{(\boldsymbol{\epsilon}, \boldsymbol{\xi}) : V(\cdot) \leq d_{s2}\}$, where $d_{s2} = \frac{1}{c_v}\left(\frac{2\rho}{c_0}\right)^{\frac{2}{2\alpha_1-1}}$. It is easily seen that $\Delta_1 \subset \Delta_2$. If an element $[\boldsymbol{\epsilon}^T, \boldsymbol{\xi}^T]^T \in \Delta_1$, from (39), it can be observed that

$$c_v V(\cdot) \leq \left(\boldsymbol{\epsilon}^T\boldsymbol{\epsilon} + \boldsymbol{\xi}^T\boldsymbol{\xi}\right) \leq \left(\frac{2\rho}{c_0}\right)^{\frac{2}{2\alpha_1-1}} \tag{43}$$

which means that the element $[\boldsymbol{\epsilon}^T, \boldsymbol{\xi}^T]^T \in \Delta_2$, and $\Delta_1 \subset \Delta_2$.
Because the augmented graph $\overline{\mathcal{G}}$ is connected, for any node v_i, there exists at least a path $\overline{L}_i$ from v_i to the leader v_0, i.e., $\overline{L}_i : v_i = v_{i_1}, v_{i_2}, \cdots, v_{i_r}, v_0$, where v_{i_r} is directly

connected with v_0. Thus, $\sqrt{\zeta}\|\boldsymbol{x}_i-\boldsymbol{x}_0\| \le \sqrt{a_{i_1i_2}}\|\boldsymbol{x}_{i_1}-\boldsymbol{x}_{i_2}\|+\cdots+\sqrt{a_{i_{r-1}i_r}}\|\boldsymbol{x}_{i_{r-1}}-\boldsymbol{x}_{i_r}\|+\sqrt{b_{i_r}}\|\boldsymbol{x}_{i_r}-\boldsymbol{x}_0\|$, where $\zeta=\min\{a_{ij},b_i,\ i,j\in\Lambda\}$. Note that

$$\begin{aligned} 2V_1(\tilde{\boldsymbol{x}}) &= \tilde{\boldsymbol{x}}^T\boldsymbol{P}_0\tilde{\boldsymbol{x}} \\ &= \sum_{i=1}^{n}\left(b_i\|\boldsymbol{x}_i-\boldsymbol{x}_0\|^2+\sum_{j}^{n}\frac{1}{2}a_{ij}\|\boldsymbol{x}_i-\boldsymbol{x}_j\|^2\right) \end{aligned} \tag{44}$$

The similar formulation can be seen in Ref. [25]. For the path $\overline{L}_i$, it can be observed that

$$\begin{aligned} \sqrt{\zeta}\|\boldsymbol{x}_i-\boldsymbol{x}_0\| &= \sqrt{\zeta}\|(\boldsymbol{x}_{i_1}-\boldsymbol{x}_{i_2})+\cdots+(\boldsymbol{x}_{i_{r-1}}-\boldsymbol{x}_{i_r})+(\boldsymbol{x}_{i_r}-\boldsymbol{x}_0)\| \\ &\le \sqrt{a_{i_1i_2}}\|\boldsymbol{x}_{i_1}-\boldsymbol{x}_{i_2}\|+\cdots+\sqrt{a_{i_{r-1}i_r}}\|\boldsymbol{x}_{i_{r-1}}-\boldsymbol{x}_{i_r}\|+\sqrt{b_r}\|\boldsymbol{x}_{i_r}-\boldsymbol{x}_0\| \\ &\le \sqrt{r}\sqrt{a_{i_1i_2}\|\boldsymbol{x}_{i_1}-\boldsymbol{x}_{i_2}\|^2+\cdots+a_{i_{r-1}i_r}\|\boldsymbol{x}_{i_{r-1}}-\boldsymbol{x}_{i_r}\|^2+b_r\|\boldsymbol{x}_{i_r}-\boldsymbol{x}_0\|^2} \\ &\le \sqrt{r}\sqrt{\sum_{i=1}^{n}\left(b_i\|\boldsymbol{x}_i-\boldsymbol{x}_0\|^2+\sum_{j}^{n}\frac{1}{2}a_{ij}\|\boldsymbol{x}_i-\boldsymbol{x}_j\|^2\right)} \\ &= \sqrt{r}\sqrt{2V_1} \le \sqrt{2n\,d_{s2}} \end{aligned} \tag{45}$$

where inequality

$$\begin{aligned} &\left(\sqrt{a_{i_1i_2}}\|\boldsymbol{x}_{i_1}-\boldsymbol{x}_{i_2}\|+\cdots+\sqrt{a_{i_{r-1}i_r}}\|\boldsymbol{x}_{i_{r-1}}-\boldsymbol{x}_{i_r}\|+\sqrt{b_r}\|\boldsymbol{x}_{i_r}-\boldsymbol{x}_0\|\right)^2 \\ &\le r^{2-1}\left(a_{i_1i_2}\|\boldsymbol{x}_{i_1}-\boldsymbol{x}_{i_2}\|^2+\cdots+a_{i_{r-1}i_r}\|\boldsymbol{x}_{i_{r-1}}-\boldsymbol{x}_{i_r}\|^2+b_r\|\boldsymbol{x}_{i_r}-\boldsymbol{x}_0\|^2\right) \end{aligned} \tag{46}$$

is used.

Inserting $\xi_{ik}=\mathrm{sgn}^{\frac{1}{\alpha_1}}(w_{ik})-\mathrm{sgn}^{\frac{1}{\alpha_1}}(w_{ik}^*)$ into $V_{2i,k}(\cdot)$ leads to

$$\begin{aligned} (\iota-w_{ik}^*)^{\frac{1}{\alpha_1}} &\le 2^{\frac{1}{\alpha_1}-1}\left(\mathrm{sgn}^{\frac{1}{\alpha_1}}(\iota)-\mathrm{sgn}^{\frac{1}{\alpha_1}}(w_{ik}^*)\right) \\ \|\boldsymbol{w}-\boldsymbol{w}^*\|^2 &\le 2^{(2-\alpha_1)(1-\alpha_1)}\sum_{i=1}^{n}\sum_{k=1}^{m}V_{2i,k}^{\alpha_1} \le 2^{(2-\alpha_1)(1-\alpha_1)}(mn)^{1-\alpha_1}V_2^{\alpha_1} \\ &\le 2^{(2-\alpha_1)(1-\alpha_1)}(mn)^{1-\alpha_1}d_{s2}^{\alpha_1} \end{aligned} \tag{47}$$

On the other side, $\tilde{\boldsymbol{v}}=(\boldsymbol{w}-\boldsymbol{w}^*)-c_3\mathrm{sgn}^{\alpha_1}(\boldsymbol{\epsilon})-\lambda\,\mathrm{sgn}^{\alpha_2}(\boldsymbol{\epsilon})$ implies

$$\begin{aligned} \|\tilde{\boldsymbol{v}}\| &\le \|\boldsymbol{w}-\boldsymbol{w}^*\|+c_3\|\mathrm{sgn}^{\alpha_1}(\boldsymbol{\epsilon})\|+\lambda\,\|\mathrm{sgn}^{\alpha_2}(\boldsymbol{\epsilon})\| \\ &\le \|\boldsymbol{w}-\boldsymbol{w}^*\|+c_3(mn)^{\frac{1-\alpha_1}{2}}\left(\boldsymbol{\epsilon}^T\boldsymbol{\epsilon}+\boldsymbol{\xi}^T\boldsymbol{\xi}\right)^{\frac{\alpha_1}{2}}+\lambda\left(\boldsymbol{\epsilon}^T\boldsymbol{\epsilon}+\boldsymbol{\xi}^T\boldsymbol{\xi}\right)^{\frac{\alpha_2}{2}} \end{aligned} \tag{48}$$

Substituting the third line of (47) into (48) results in

$$\|\boldsymbol{v}_i-\boldsymbol{v}_0\| \le \left(2^{\frac{(2-\alpha_1)(1-\alpha_1)}{2}}+c_3c_v^{\frac{\alpha_1}{2}}\right)(mn)^{\frac{1-\alpha_1}{2}}d_{s2}^{\frac{\alpha_1}{2}}+\lambda\,c_v^{\frac{\alpha_2}{2}}d_{s2}^{\frac{\alpha_2}{2}} \tag{49}$$

It is obvious that, if the state vector $[\boldsymbol{x}_i^T,\boldsymbol{v}_i^T]^T$ satisfies inequalities (45) and (49), $[\boldsymbol{x}_i^T,\boldsymbol{v}_i^T]^T\in\mathcal{S}_i$ will be met at the same time.

The proof is complete. □

Then, consider the MAS (9), (10) and (19) operating in the time interval $t\in[0,T_1]$. What needs to be done is that the boundedness for each agent states must be guaranteed. Stability analysis of the closed-loop system (9), (11) and (19) is very cumbersome when the system operates in the time interval $t\in[0,T_1]$. Therefore, a simpler linear distributed

control (LDC) law is employed to take the place of (19). During $t \in [0, T_1]$, the adopted LDC law is presented as

$$\boldsymbol{u}_i = -\sum_{j \in N_i} a_{ij}(\boldsymbol{x}_i - \boldsymbol{x}_j) - c_6 \boldsymbol{v}_i \tag{50}$$

Concerning the closed-loop system (9), (10), and (50), the states of each agent are bounded during $t \in [0, T_1]$. Choose another Lyapunov-function candidate as

$$V_3(\boldsymbol{x}, \boldsymbol{v}) = \frac{1}{2}\boldsymbol{x}^T \boldsymbol{P}_1 \boldsymbol{x} + \frac{1}{2}\boldsymbol{v}^T \boldsymbol{v} \tag{51}$$

where $\boldsymbol{x} = [\boldsymbol{x}_1, \cdots, \boldsymbol{x}_n]^T \in \mathcal{R}^{mn}$, $\boldsymbol{v} = [\boldsymbol{v}_1, \cdots, \boldsymbol{v}_n]^T \in \mathcal{R}^{mn}$, and $\boldsymbol{P}_1 = \boldsymbol{L} \otimes \boldsymbol{I}_m$. Differentiating $V_3(\cdot)$ along (9), (10) and (50) results in

$$\begin{aligned} \dot{V}_3(\cdot) &= -c_6 \boldsymbol{v}^T \boldsymbol{v} + \boldsymbol{v}^T \boldsymbol{d} \\ &\leq -[(c_6 - \frac{1}{2})\boldsymbol{v}^T \boldsymbol{v} - \frac{1}{2} n D_0^2] \end{aligned} \tag{52}$$

When $\|\boldsymbol{v}\| \geq \sqrt{\frac{n}{2c_6 - 1}}\, D_0$, $\dot{V}_3$ is negative-definite. This also indicates that $\|\boldsymbol{v}_i\| \leq \|\boldsymbol{v}\| \leq b_v$, where $b_v = \min\{\boldsymbol{v}(0), \sqrt{\frac{n}{2c_6 - 1}}\, D_0\}$, $\boldsymbol{v}(0)$ is the initial value of $\boldsymbol{v}$. It follows that

$$\|\dot{\boldsymbol{x}}_i\| \leq \|\boldsymbol{v}_i\| \leq b_v \tag{53}$$

which implies that

$$\|\boldsymbol{x}_i\|(t) \leq b_v t + \|\boldsymbol{x}_i\|(0) \leq b_v T_1 + \|\boldsymbol{x}_i\|(0),\ t \in [0, T_1) \tag{54}$$

Therefore, in accordance with (54) and $\|\boldsymbol{v}_i\| \leq b_v$, it could be observed that, if $c_6 \geq \frac{1}{2}$, the state vector $[\boldsymbol{x}_i^T, \boldsymbol{v}_i^T]^T$ of the i-th agent is bounded in the time interval $t \in [0, T_1]$.

Ultimately, combining the DFCTC law (19) with the LDC law (50), a distributed attitude consensus tracking controller for the i-th rigid-body of the MAS (9) is formulated as

$$\begin{cases} \boldsymbol{u}_i = -\sum\limits_{j \in N_i} a_{ij}(\boldsymbol{\chi}_i - \boldsymbol{\chi}_j) - c_6 \dot{\boldsymbol{\chi}}_i,\ 0 \leq t < T_1 \\ \boldsymbol{u}_i = -c_4\, \mathrm{sgn}^{2\alpha_1 - 1}\left\{ \mathrm{sgn}^{\frac{1}{\alpha_1}}[(\boldsymbol{v}_i - \hat{\boldsymbol{v}}_i) + \lambda\, \mathrm{sgn}^{\alpha_2}(\boldsymbol{\epsilon}_i)] + c_3^{\frac{1}{\alpha_1}} \boldsymbol{\epsilon}_i \right\} \\ \qquad - c_5\, \mathrm{sgn}^{\alpha_1 + \alpha_2 - 1}\left\{ \mathrm{sgn}^{\frac{1}{\alpha_1}}[(\boldsymbol{v}_i - \hat{\boldsymbol{v}}_i) + \lambda\, \mathrm{sgn}^{\alpha_2}(\boldsymbol{\epsilon}_i)] + c_3^{\frac{1}{\alpha_1}} \boldsymbol{\epsilon}_i \right\} \\ \qquad - \lambda \alpha_2\, \mathrm{diag}\{|\boldsymbol{\epsilon}_i|^{\alpha_2 - 1}\} \boldsymbol{\eta}_i,\ t \geq T_1 \\ \boldsymbol{\tau}_i = \boldsymbol{\Pi}_i \boldsymbol{u}_i \end{cases} \tag{55}$$

where $\boldsymbol{\epsilon}_i = \sum_{j \in N_i} a_{ij}(\boldsymbol{\chi}_i - \boldsymbol{\chi}_j) + b_i(\boldsymbol{\chi}_i - \boldsymbol{\chi}_0)$, $\boldsymbol{v}_i = \dot{\boldsymbol{\chi}}_i$, $\boldsymbol{\eta}_i = \sum_{j \in N_i} a_{ij}(\dot{\boldsymbol{\chi}}_i - \dot{\boldsymbol{\chi}}_j) + b_i(\dot{\boldsymbol{\chi}}_i - \dot{\boldsymbol{\chi}}_0)$. $\hat{\boldsymbol{v}}_i$ is the estimation of $\dot{\boldsymbol{\chi}}_0$ for the i-th rigid-body, where the REDFTO (11) is used.

Remark 3. *For second-order MASs in the presence of uncertainties, different robust distributed fixed-time consensus control laws have been proposed [28,29,31]. In comparison with those works, some significant improvements are acquired in Theorem 2. In Ref. [28,29], to mitigate chattering effects, the saturation-function and boundary-layer techniques are used, which will degrade performance on control precision of the closed-loop system. For the proposed DFCTC law, by properly choosing the parameter $\frac{1}{2} < \alpha_1 < 1$, continuous control signals are obtained without use of the saturation-function technique. In Ref. [31], the settling-time could not be explicitly estimated due to employment of the bi-limit homogeneity technique. In Theorem 2, by means of the modified back-stepping technique and the adding of a power integrator technique [32], the settling-time could be explicitly given. Moreover, as is stated in Theorem 2, the ultimate boundary of the consensus tracking error for each agent is explicitly provided.*

Remark 4. *Seeing that the settling-time T_1 of REDFTO could be prescribed by the designer, the control strategy, which switches from (50) to (19) when $t > T_1$, is entirely feasible. A similar strategy could be found in Ref. [25,35]. However, in Ref. [25,35], the control strategy is actually difficult to implemented. Because the presented observer in Ref. [25,35] is finite-time convergence, the settling-time is dependent on the initial value, which may be unknown beforehand. This deficiency can be improved in this paper.*

Remark 5. *It must be pointed out that estimation of T_2 is more conservative due to the use of inequality (25). Some improvements are needed in future work.*

4. Simulations

Consider a team of five rigid-bodies, which includes a virtual-leader. The information interaction is depicted in Figure 1, where the weighted adjacency matrix $\boldsymbol{A}$ and $\boldsymbol{B}$ are expressed as

$$\boldsymbol{A} = \begin{bmatrix} 0 & 1 & 0 & 1 \\ 1 & 0 & 1 & 0 \\ 0 & 1 & 0 & 1 \\ 1 & 0 & 1 & 0 \end{bmatrix}, \ \boldsymbol{B} = \begin{bmatrix} 0 & 0 & 0 & 0 \\ 0 & 2 & 0 & 0 \\ 0 & 0 & 0 & 0 \\ 0 & 0 & 0 & 2 \end{bmatrix} \tag{56}$$

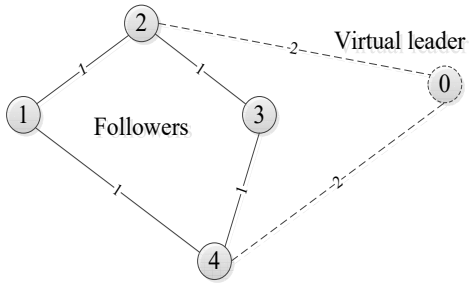

Figure 1. Communication topology of the augmented graph.

To further illustrate the proposed control scheme, two control principle block-diagrams are presented as below:

When the running time is during the time-interval $t \leq T_1$, a control scheme is shown in Figure 2. When the running time is during the time-interval $t \geq T_1$, a control scheme is depicted in Figure 3. Note that, if the follower could access all states of the virtual-leader directly (i.e., the parameter $b_i > 0$), the REDFT observer is not necessary.

To show the superiority of the proposed DFCTC law, a comparison study is carried out between the proposed DFCTC and the finite-time consensus algorithm (FTCA) for leader–follower MASs. The compared algorithm was proposed by the authors of [25], which has several properties similar to the proposed DFCTC, e.g., robustness against unknown uncertainties and high control accuracy.

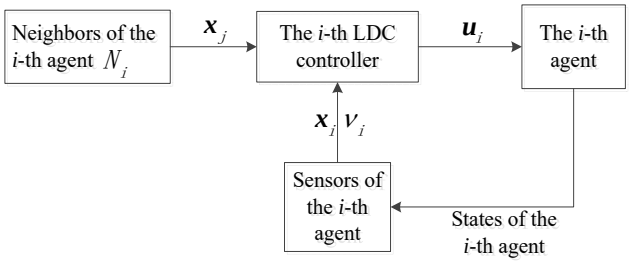

Figure 2. Control principle block-diagram of the presented LDC law.

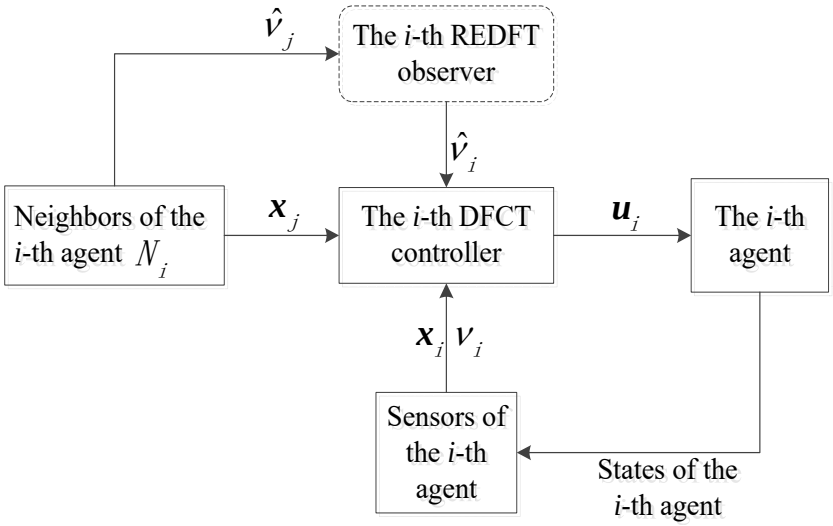

Figure 3. Control principle block-diagram of the proposed DFCTC law.

Parameters of REDFTO (11) are listed in Table 1. Parameters of the proposed DFCTC law and the compared FTCA law are listed in Table 2. According to (18) and Table 1, convergence time T_1 of the REDFTO (11) is $T_1 = 0.66$.

Table 1. Parameters of the REDFTO.

Parameter	c_1	c_2	β
Value	16	200	1.5

Table 2. Parameters of the DFCTC and the FTCA.

Controller	**Parameters**						
DFCTC	λ	c_3	c_4	c_5	c_6	α_1	α_2
	2	2	80	80	2	0.8	1.1
FTCA	k_1	k_2	p				
	80	1.8	5/4				

The reference attitude acceleration profile is set to $\boldsymbol{u}_0 = [\cos t, \sin t, \frac{1}{2}(\cos t + \sin t)]^T$, rad/s^2. The lumped disturbances acting on each rigid-body are set to $\boldsymbol{d}_1(\cdot) = \boldsymbol{d}_2(\cdot) = \boldsymbol{d}_3(\cdot) = \boldsymbol{d}_4(\cdot) = [\cos 0.5t, \sin 0.5t, \cos 0.5t + \sin 0.5t]^T$, rad/s^2. Simulation results are shown in Figures 4–9.

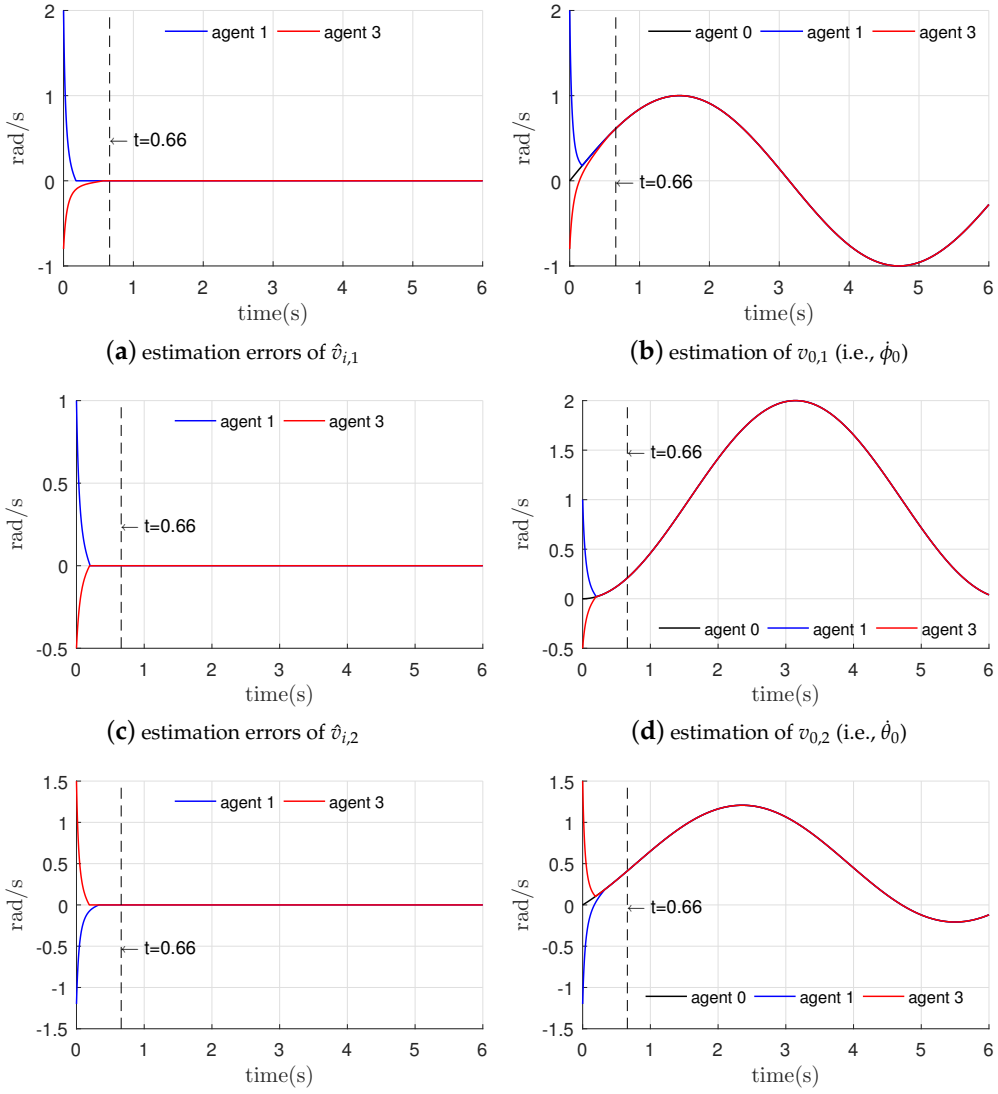

(**a**) estimation errors of $\hat{v}_{i,1}$ (**b**) estimation of $v_{0,1}$ (i.e., $\dot{\phi}_0$)

(**c**) estimation errors of $\hat{v}_{i,2}$ (**d**) estimation of $v_{0,2}$ (i.e., $\dot{\theta}_0$)

(**e**) estimation errors of $\hat{v}_{i,3}$ (**f**) estimation of $v_{0,3}$ (i.e., $\dot{\psi}_0$)

Figure 4. Estimation errors of the REDFTO for agents $i = 1$ and $i = 3$.

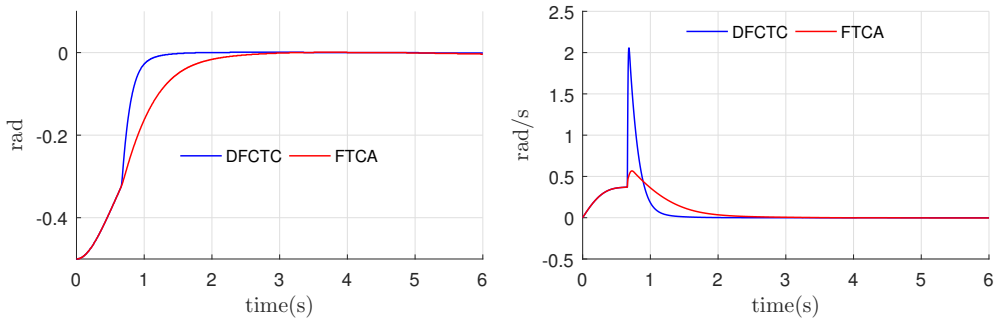

(**a**) consensus tracking errors of ϕ_1 (**b**) consensus tracking errors of $\dot{\phi}_1$

Figure 5. *Cont.*

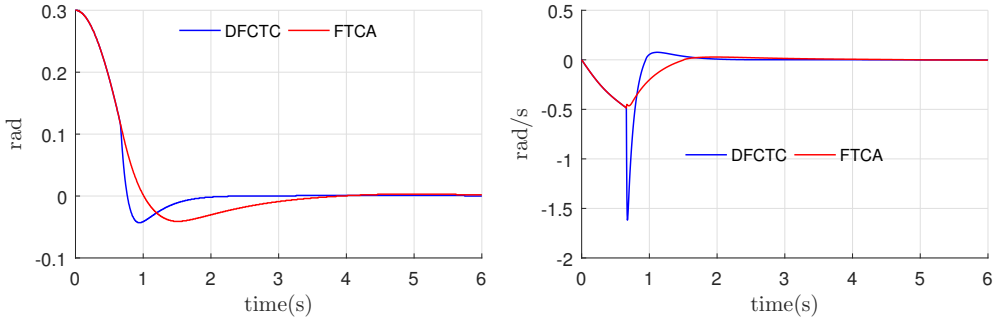

(**c**) consensus tracking errors of θ_1 (**d**) consensus tracking errors of $\dot{\theta}_1$

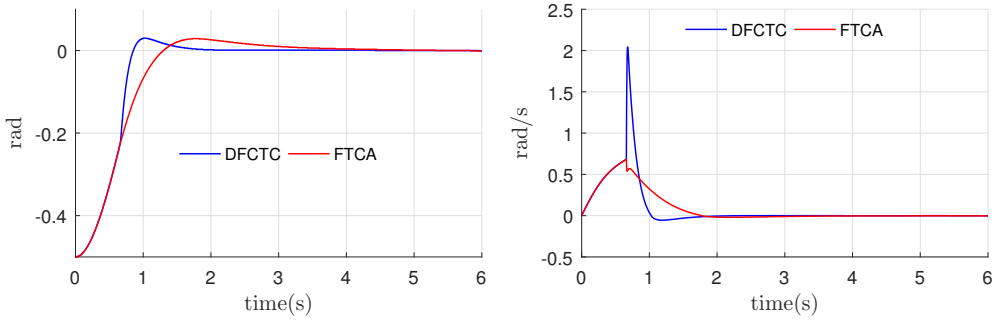

(**e**) consensus tracking errors of ψ_1 (**f**) consensus tracking errors of $\dot{\psi}_1$

Figure 5. Consensus tracking errors for agent $i = 1$.

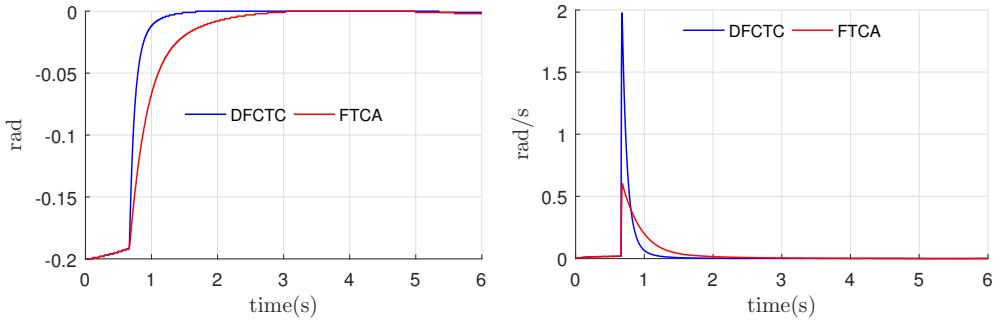

(**a**) consensus tracking errors of ϕ_2 (**b**) consensus tracking errors of $\dot{\phi}_2$

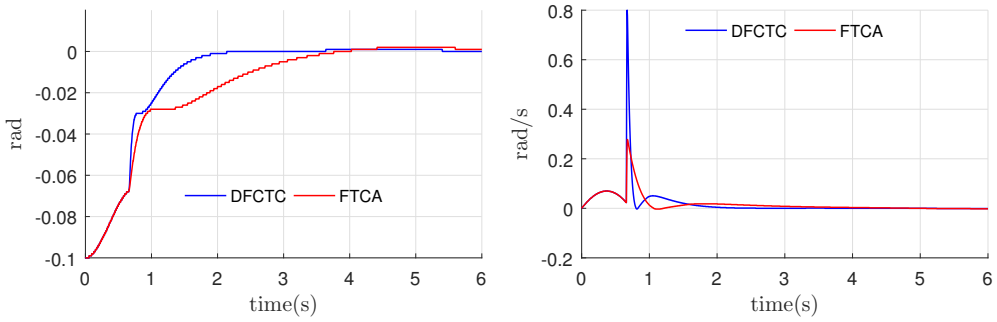

(**c**) consensus tracking errors of θ_2 (**d**) consensus tracking errors of $\dot{\theta}_2$

Figure 6. *Cont.*

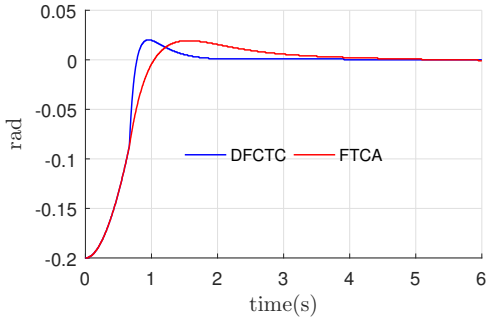

(e) consensus tracking errors of ψ_2

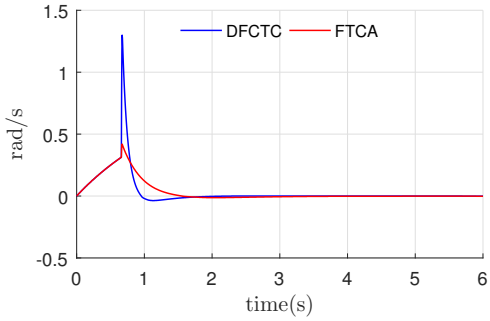

(f) consensus tracking errors of $\dot{\psi}_2$

Figure 6. Consensus tracking errors for agent $i = 2$.

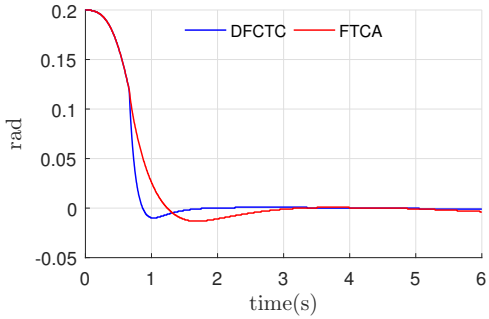

(a) consensus tracking errors of ϕ_3

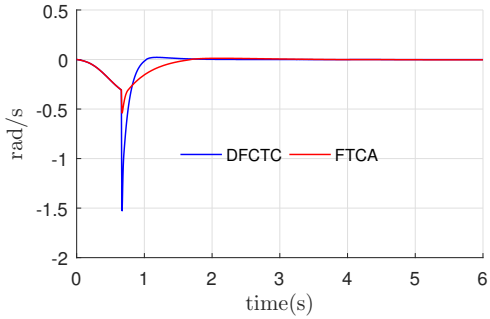

(b) consensus tracking errors of $\dot{\phi}_3$

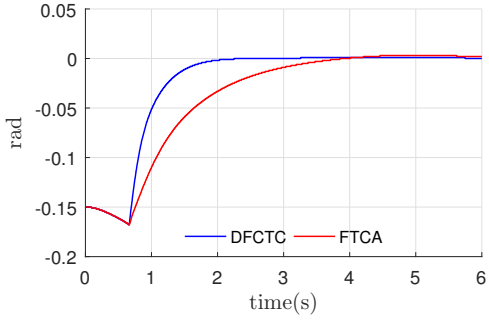

(c) consensus tracking errors of θ_3

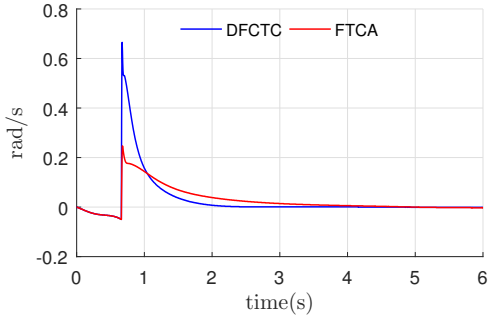

(d) consensus tracking errors of $\dot{\theta}_3$

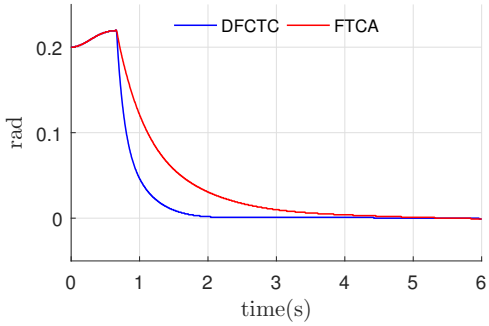

(e) consensus tracking errors of ψ_3

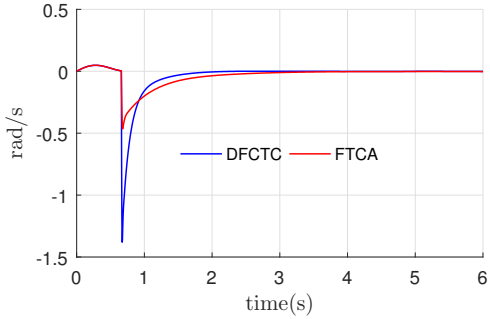

(f) consensus tracking errors of $\dot{\psi}_3$

Figure 7. Consensus tracking errors for agent $i = 3$.

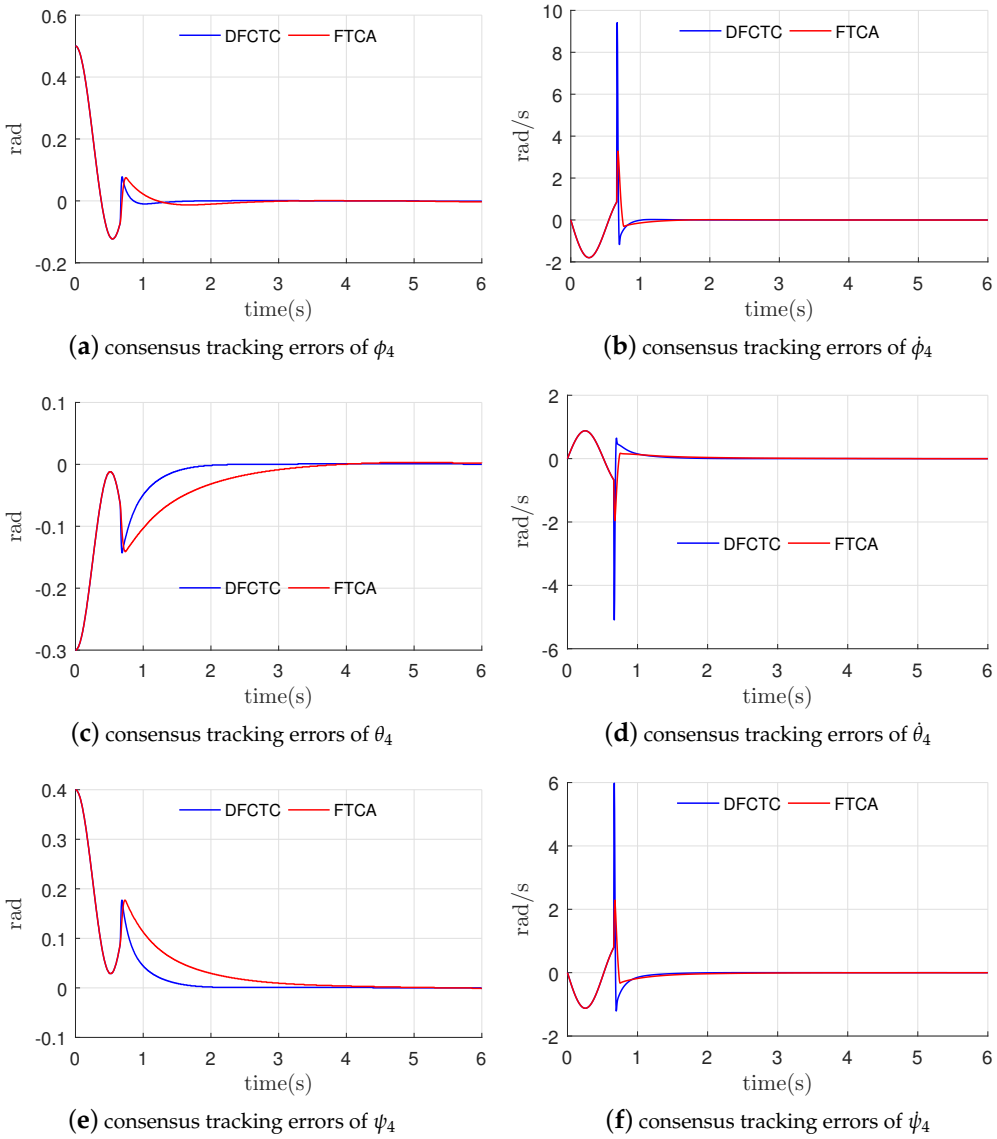

(**a**) consensus tracking errors of ϕ_4 (**b**) consensus tracking errors of $\dot{\phi}_4$

(**c**) consensus tracking errors of θ_4 (**d**) consensus tracking errors of $\dot{\theta}_4$

(**e**) consensus tracking errors of ψ_4 (**f**) consensus tracking errors of $\dot{\psi}_4$

Figure 8. Consensus tracking errors for agent $i = 4$.

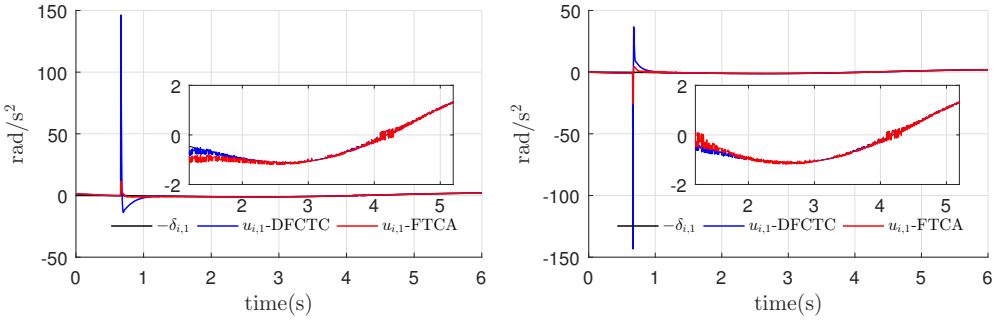

(**a**) control signal $u_{i,1}$ and the disturbance $-\delta_{i,1}$ for $i = 1$ (**b**) control signal $u_{i,1}$ and the disturbance $-\delta_{i,1}$ for $i = 3$

Figure 9. *Cont.*

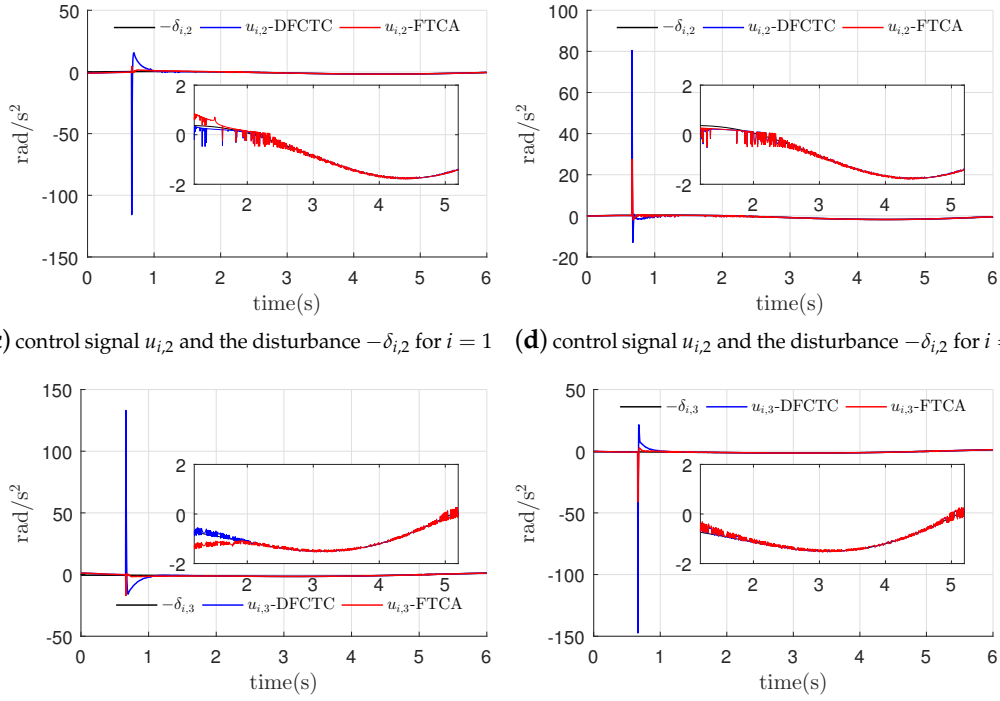

(c) control signal $u_{i,2}$ and the disturbance $-\delta_{i,2}$ for $i = 1$ **(d)** control signal $u_{i,2}$ and the disturbance $-\delta_{i,2}$ for $i = 3$

(e) control signal $u_{i,3}$ and the disturbance $-\delta_{i,3}$ for $i = 1$ **(f)** control signal $u_{i,3}$ and the disturbance $-\delta_{i,3}$ for $i = 3$

Figure 9. Control signals and disturbances for agents $i = 1, 3$.

In Figure 4a,c,e, it could be seen that estimation errors of the REDFTO converge to zero in a fixed-time. Therefore, the REDETOs for $i = 1$, $i = 3$ could estimate velocity state of the virtual-leader exactly after $t = 0.66$, which could be easily seen in Figure 4b,d,f.

Note that, during the time interval $t \in [0, 0.66)$, the used control law is the LDC law expressed in the first line of (55). When the time is greater than 0.66, the used control law is the DFCTC expressed in the second line of (55) (the blue lines) or the FTCA proposed in [25] (the red lines). As illustrated in Figures 5–8, when the proposed DFCTC is adopted, the attitude consensus tracking is achieved in a fixed-time. Obviously, convergence speed of the DFCTC is faster than that of the FTCA. The reason is that the settling-time of the DFCTC is independent of the initial conditions. However, settling-time of the FTCA is dependent of the initial conditions.

In Figure 9, it is easily observed that the value of the control signal $\boldsymbol{u}_i$ is almost equal to the opposite value of the disturbance $\boldsymbol{\delta}_i(\cdot)$ after the time $t = 3.0$ s. What this means is that the control signal could largely compensate the disturbance when the consensus tracking errors enter a small bounded set around the origin. Note that the overall disturbance $\boldsymbol{\delta}_i(\cdot)$, which is expressed as $\boldsymbol{\delta}_i(\cdot) = \boldsymbol{d}_i(\cdot) - \dot{\boldsymbol{v}}_0$, consists of two parts: uncertainty $\boldsymbol{d}_i(\cdot)$ acting on the i-th rigid-body and acceleration of the virtual-leader $\dot{\boldsymbol{v}}_0$. $u_{i,1}$, $u_{i,2}$, $u_{i,3}$ are three components of $\boldsymbol{u}_i$ (i.e., $\boldsymbol{u}_i = [u_{i,1}, u_{i,2}, u_{i,3}]^T$), and $\delta_{i,1}$, $\delta_{i,2}$, $\delta_{i,3}$ are three components of $\boldsymbol{\delta}_i$ (i.e., $\boldsymbol{\delta}_i = [\delta_{i,1}, \delta_{i,2}, \delta_{i,3}]^T$).

In Figure 9, at the time instant $t = T_1 = 0.66$ s, the control signals are slightly larger. This is because the control law is switched from the LDC law to the DFCTC law at the time instant $t = 0.66$ s.

5. Conclusions

The attitude consensus tracking problem has been investigated for a group of multiple rigid-bodies with time-varying uncertainty acting on each agent. The reference command profile has been seen as a virtual-leader, and a REDFTO used to estimate velocity state of the virtual-leader has been developed. Subsequently, a DFCTC law has been proposed. Fixed-time convergence of the tracking errors to a bounded region including the origin has

been analytically proved. In the simulation section, a comparison case study confirms the effectiveness and superiority of the proposed control scheme.

However, there are some limitations with the proposed DFCTC law. As stated in Remark 5, estimation of the convergence time T_2 is more conservative. From the simulation results, when in the time interval $t < T_1$, the DFCTC law is not used. These two limitations must be improved in the future work.

Author Contributions: Conceptualization, S.J., Z.Y. and Y.G.; methodology, S.J. and Y.G.; software, S.J. and C.X.; validation, S.J., H.X. and C.X.; formal analysis, S.J. and Y.G.; investigation, S.J. and Y.G.; resources, S.J. and Z.Y.; data curation, S.J.; writing—original draft preparation, S.J. and Y.G.; writing—review and editing, S.J. and Y.G.; visualization, S.J.; supervision, Z.Y.; funding acquisition, Z.Y. All authors have read and agreed to the published version of the manuscript.

Funding: This work was supported by the National Natural Science Foundation of China (Grant No. 61473144).

Data Availability Statement: The figures, tables, and other data used to support this study are included within the article.

Acknowledgments: The authors would like to thank the anonymous reviewers for their precious comments that helped us to improve the presentation of our results. The authors would also like to thank the associate editor for the time spent and the effort made in the reviewing process.

Conflicts of Interest: The authors declare that they have no known competing financial interest or personal relationships that could have appeared to influence the work reported in this paper.

References

1. Liu, Y.; Jiang, B.; Lu, J.; Cao, J.; Lu, G. Event-triggered sliding mode control for attitude stabilization of a rigid spacecraft. *IEEE Trans. Syst. Man Cybern. Syst.* **2020**, *50*, 3290–3299. [CrossRef]
2. Jiang, S.; Liu, C.S.; Gao, Y.X. MIMO Adaptive High-Order Sliding Mode Control for Quadrotor Attitude Tracking. *J. Aerosp. Eng.* **2021**, *34*, 04021022. [CrossRef]
3. Wang, H.; Peter, L.; Zhao, X.; Liu, X. Adaptive fuzzy finite-time control of nonlinear systems with actuator faults. *IEEE Trans. Cybern.* **2020**, *50*, 1786–1797. [CrossRef] [PubMed]
4. Bajrami, X.; Pajaziti, A.; Likaj, R.; Shala, A.; Berisha, R.; Bruqi, M. Control theory application for swing up and stabilisation of rotating inverted pendulum. *Symmetry* **2021**, *13*, 1491. [CrossRef]
5. Qiu, B.; Wang, G.; Fan, Y.; Mu, D.; Sun, X. Adaptive sliding mode trajectory tracking control for unmanned surface vehicle with modeling uncertainties and input saturation. *Appl. Sci.* **2019**, *9*, 1240. [CrossRef]
6. Zheng, Z.; Xu, Y.; Zhang, L.S.; Song, S.M. Decentralized attitude synchronization tracking control for multiple spacecraft under directed communication topology. *Chin. J. Aeronaut.* **2016**, *29*, 995–1006. [CrossRef]
7. Chung, S.J.; Ahsun, U.; Slotine, J.E. Application of synchronization to formation flying spacecraft: Lagrangian approach. *J. Guid. Control Dyn.* **2009**, *32*, 512–526. [CrossRef]
8. Xiao, M.; Liu, Z.T.; Su, H.Y. Distributed event-triggered adaptive control for second-order nonlinear uncertain multi-agent systems. *Chin. J. Aeronaut.* **2021**, *34*, 237–247. [CrossRef]
9. Liu, H.; Cheng, L.; Tan, M.; Hou, Z. Exponential finite-time consensus of fractional-order multiagent systems. *IEEE Trans. Syst. Man Cybern. Syst.* **2020**, *50*, 1549–1558. [CrossRef]
10. Cai, H.; Huang, J. The leader-following attitude control of multiple rigid spacecraft systems. *Automatica* **2014**, *50*, 1109–1115. [CrossRef]
11. Ren, W. Distributed attitude synchronization and tracking control for multiple rigid bodies. *IEEE Trans. Contrl Syst. Technl.* **2010**, *18*, 383–392. [CrossRef]
12. Rekabi, F.; Shirazi, F.A.; Sadigh, M.J. Distributed nonlinear H_∞ control algorithm for multi-agent quadrotor formation flying. *ISA Trans.* **2020**, *96*, 81–94. [CrossRef] [PubMed]
13. Zhou, P.P.; Chen, B.M. Semi-global leader-following consensus-based formation flight of unmanned aerial vehicles. *Chin. J. Aeronaut.* **2021**, *34*, in press. [CrossRef]
14. Zhou, W.H.; Li, J.; Liu, Z.H.; Shen, L.C. Improving multi-target cooperative tracking guidance for UAV swarms using multi-agent reinforcement learning. *Chin. J. Aeronaut.* **2021**, *34*, in press. [CrossRef]
15. Han, L.; Dong, X.W.; Li, Q.D.; Ren, Z. Formation tracking control for time-delayed multi-agent systems with second-order dynamics. *Chin. J. Aeronaut.* **2017**, *30*, 348–357. [CrossRef]
16. Peng, Z.X.; Wen, G.G.; Yang, S.C.; Rahmani, A. Distributed consensus-based formation control for nonholonomic wheeled mobile robots using adaptive neural network. *Nonlinear Dyn.* **2016**, *86*, 605–622. [CrossRef]

17. Guo, S.P.; Li, Z.K.; Niu, Y.F.; Wu, L.Z. Consensus disturbance rejection control of directed multi-agent networks with extended state observer. *Chin. J. Aeronaut.* **2020**, *33*, 1486–1493. [CrossRef]
18. Long, T.; Cao, Y.; Sun, J.L.; Xu, G.T. Adaptive event-triggered distributed optimal guidance design via adaptive dynamic programming. *Chin. J. Aeronaut.* **2021**, *34*, in press. [CrossRef]
19. Sun, J.L.; Long, T. Event-triggered distributed zero-sum differential game for nonlinear multi-agent systems using adaptive dynamic programming. *ISA Trans.* **2021**, *110*, 39–52. [CrossRef]
20. Sun, J.L.; Liu, C.S. Distributed fuzzy adaptive backstepping optimal control for nonlinear multimissile guidance systems with input saturation. *IEEE Trans. Fuzzy Syst.* **2019**, *27*, 447–461. [CrossRef]
21. Abdessameud, A.; Tayebi, A. Attitude synchronization of a group of spacecraft without velocity measurements. *IEEE Trans. Autom. Control* **2009**, *54*, 2642–2648. [CrossRef]
22. Hua, C.C.; Li, K.; Guan, X.P. Leader-following output consensus for high-rrder nonlinear multiagent systems. *IEEE Trans. Autom. Control* **2019**, *64*, 1156–1161. [CrossRef]
23. Li, X.W.; Soh, Y.C.; Xie, L.H. A novel reduced-order protocol for consensus control of linear multiagent systems. *IEEE Trans. Autom. Control* **2019**, *64*, 3005–3012. [CrossRef]
24. Zou, A.M.; De Ruiter, A.; Kumar, K.D. Distributed finite-time velocity-free attitude coordination control for spacecraft formations. *Automatica* **2016**, *67*, 46–53. [CrossRef]
25. Li, S.H.; Du, H.B.; Lin, X.Z. Finite-time consensus algorithm for multi-agent systems with double-integrator dynamics. *Automatica* **2011**, *47*, 1706–1712. [CrossRef]
26. Zheng, S.Q.; Ahn, C.K.; Shi, P.; Xie, Y.L. Prescribed finite-time consensus with severe unknown nonlinearities and mismatched disturbances. *Syst. Control Lett.* **2021**, *157*, 105047. [CrossRef]
27. Zuo, Z.Y.; Han, Q.L.; Ning, B.D.; Ge, X.H.; Zhang, X.M. An overview of recent advances in fixed-time cooperative control of multiagent systems. *IEEE Trans. Ind. Informat.* **2018**, *14*, 2322–2334. [CrossRef]
28. Fu, J.J.; Wang, J.Z. Fixed-time coordinated tracking for second-order multi-agent systems with bounded input uncertainties. *Syst. Control Lett.* **2016**, *93*, 1–12. [CrossRef]
29. Xu, C.; Wu, B.L.; Wang, D.W.; Zhang, Y.C. Distributed fixed-time output-feedback attitude consensus control for multiple spacecraft. *IEEE Trans. Aerosp. Electron. Syst.* **2020**, *56*, 4779–4795. [CrossRef]
30. Cruz-Zavala, E.; Moreno, J.A. Homogeneous High Order Sliding Mode design: A Lyapunov approach. *Automatica* **2017**, *80*, 232–238. [CrossRef]
31. Tian, B.L.; Lu, H.C.; Zuo, Z.Y.; Yang, W. Fixed-time leader–follower output feedback consensus for second-order multiagent systems. *IEEE Trans. Cybern.* **2019**, *49*, 1545–1550. [CrossRef] [PubMed]
32. Qian, C.J.; Lin, W. A continuous feedback approach to global strong stabilization of nonlinear systems. *IEEE Trans. Autom. Control* **2001**, *46*, 1061–1079. [CrossRef]
33. Ding, S.H.; Li, S.H.; Zheng, W.X. Nonsmooth stabilization of a class of nonlinear cascaded systems. *Automatica* **2012**, *48*, 2597–2606. [CrossRef]
34. Kun, D.W.; Hwang, I. Linear matrix inequality-based nonlinear adaptive robust control of quadrotor. *J. Guid. Control Dyn.* **2016**, *39*, 996–1008. [CrossRef]
35. Meng, Z.Y.; Ren, W.; You, Z. Distributed finite-time attitude containment control for multiple rigid bodies. *Automatica* **2010**, *46*, 2092–2099. [CrossRef]